

# Pembrolizumab plus axitinib versus sunitinib for advanced clear cell renal cell carcinoma: 5-year survival and biomarker analyses of the phase 3 KEYNOTE-426 trial

---

Received: 22 January 2025

---

Accepted: 27 June 2025

---

Published online: 01 August 2025

---

 Check for updates

---

---

A list of authors and their affiliations appears at the end of the paper

---

At the first interim analysis of the phase 3 KEYNOTE-426 trial, first-line pembrolizumab plus axitinib showed superior overall survival (OS), progression-free survival (PFS) and objective response rate (ORR) over sunitinib for advanced renal cell carcinoma (RCC). To assess long-term durability of clinical outcomes and elucidate predictive biomarkers for RCC, we performed efficacy and prespecified exploratory biomarker analyses from KEYNOTE-426 with  $\geq 5$  years of follow-up. Pembrolizumab plus axitinib showed sustained benefits in OS (hazard ratio: 0.84; 95% confidence interval: 0.71–0.99), PFS (hazard ratio: 0.69; 95% confidence interval: 0.59–0.81) and ORR (60.6% versus 39.6%) compared to sunitinib. An 18-gene T-cell-inflamed gene expression profile (Tcell<sub>inf</sub>GEP) was positively associated with OS ( $P = 0.002$ ), PFS ( $P < 0.0001$ ) and ORR ( $P < 0.0001$ ) within the pembrolizumab plus axitinib arm. An angiogenesis signature was positively associated with OS ( $P = 0.004$ ) within the pembrolizumab plus axitinib arm and with OS ( $P < 0.0001$ ), PFS ( $P < 0.001$ ) and ORR ( $P = 0.002$ ) within the sunitinib arm. Across arms, programmed cell death ligand 1 combined positive score was only associated (negatively) with OS within the sunitinib arm ( $P = 0.025$ ). Additionally, *PBRM1* (polybromo-1) mutation had a positive association with ORR ( $P = 0.002$ ) within the pembrolizumab plus axitinib arm. Within the sunitinib arm, OS was positively associated with *VHL* (von Hippel–Lindau tumor suppressor gene) ( $P = 0.040$ ) and *PBRM1* ( $P = 0.010$ ) mutations and was negatively associated with *BAP1* (*BRCA1*-associated protein 1) mutation ( $P = 0.019$ ). Results showed a sustained clinical benefit with pembrolizumab plus axitinib over sunitinib and provide valuable information on biomarkers for immunotherapy-based treatment combinations in advanced RCC. Prospective clinical investigations are needed for biomarker-directed treatment for advanced RCC. ClinicalTrials.gov identifier: [NCT02853331](https://clinicaltrials.gov/ct2/show/study/NCT02853331).

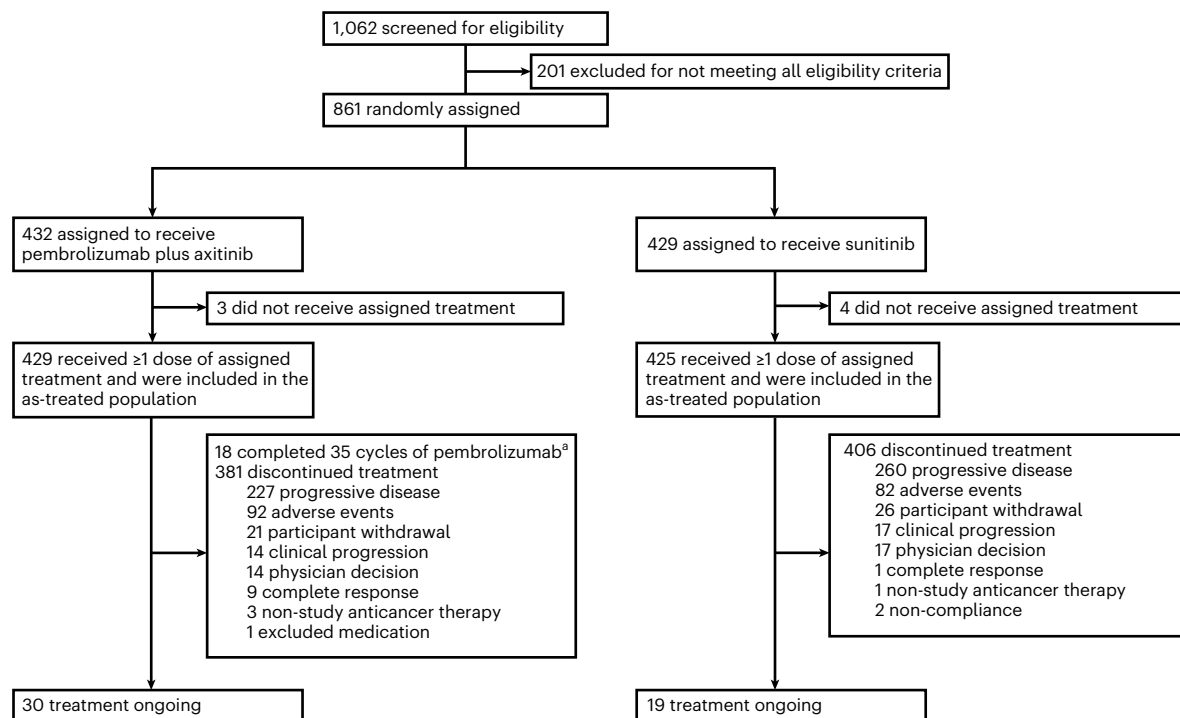


**Fig. 1 | CONSORT diagram.** <sup>a</sup>Completed pembrolizumab treatment after discontinuing axitinib.

The combination of the programmed cell death protein 1 (PD-1) inhibitor pembrolizumab and the vascular endothelial growth factor receptor (VEGFR) tyrosine kinase inhibitor (TKI) axitinib is standard-of-care first-line treatment for patients with advanced clear cell RCC, as a result of outcomes from the open-label, randomized, phase 3 KEYNOTE-426 trial<sup>1–5</sup>. KEYNOTE-426 was the first trial of a PD-1 inhibitor and VEGFR-TKI combination in the first-line treatment setting and, therefore, has the longest follow-up duration of any combination of a PD-1 or programmed cell death ligand 1 (PD-L1) inhibitor and a TKI. Because the treatment duration of pembrolizumab is limited to 2 years, it is important to assess the long-term durability of clinical outcomes.

There is an unmet need for biomarkers that are predictive of patient outcomes after using available first-line treatment options in RCC<sup>6,7</sup>. Studies to evaluate predictive and prognostic biomarkers in metastatic RCC have been largely derived from phase 3 studies (for example, IMmotion151, JAVELIN Renal 101 and Check-Mate 9ER) in which similar mechanisms (for example, PD-L1 inhibitor plus VEGF-TKI) but different drugs were evaluated as frontline therapy<sup>8–22</sup>. Thus, extrapolation of these data to define predictive biomarkers in frontline therapy for advanced RCC is potentially confounded. Nonetheless, the studies yielded relevant biological insight into the role of molecular features of RCC, including PD-L1 expression, interferon gamma (IFN $\gamma$ ) RNA signatures, specific DNA alterations (such as *PBRM1* mutations), mRNA-based molecular clusters, circulating kidney injury molecule-1 (KIM-1) and serum glycopeptides<sup>8–11,14,17,19–22</sup>. Further investigation is warranted to identify tumor and (or) stromal biologic features that may define susceptible patient populations.

Here we report the final clinical data after 5 years of follow-up from KEYNOTE-426 and the results of a prespecified exploratory biomarker analysis that was conducted to determine whether molecular determinants relevant to the underlying disease biology are associated with clinical outcomes (ORR, PFS and OS) for pembrolizumab plus axitinib and for sunitinib in participants with advanced clear cell RCC.

## Results

### Participants

Between 24 October 2016 and 24 January 2018, 861 participants were randomly assigned to receive either pembrolizumab plus axitinib ( $n = 432$ ) or sunitinib monotherapy ( $n = 429$ ) (Fig. 1). As of the data cutoff date, the median follow-up (defined as time from randomization to the database cutoff date for this exploratory analysis) was 67.2 months (range, 60.0–75.0 months). Baseline demographics and characteristics are shown in Table 1. A total of 429 participants in the pembrolizumab plus axitinib arm and 425 participants in the sunitinib arm received at least one dose of the assigned study treatment. At the time of this analysis, 381 of 429 treated participants (88.8%) in the pembrolizumab plus axitinib arm and 406 of 425 treated participants (95.5%) in the sunitinib arm had permanently discontinued study treatment, most commonly due to radiographic progressive disease (pembrolizumab plus axitinib,  $n = 227$  (52.9%); sunitinib,  $n = 260$  (61.2%)) (Fig. 1). Thirty of 429 participants (7.0%) in the pembrolizumab plus axitinib arm and 19 of 425 participants (4.5%) in the sunitinib arm remained on treatment.

Among participants who discontinued study treatment, 237 of 381 (62.2%) in the pembrolizumab plus axitinib arm and 300 of 406 (73.9%) in the sunitinib arm received subsequent systemic anticancer therapy, most commonly a VEGFR inhibitor in the pembrolizumab plus axitinib arm (206/237 (86.9%)) and a PD-L1 inhibitor in the sunitinib arm (240/300 (80.0%)) (Supplementary Table 1).

### Efficacy outcomes

By the data cutoff date, 550 participants in the intention-to-treat population had died, including 270 of 432 participants (62.5%) in the pembrolizumab plus axitinib arm and 280 of 429 participants (65.3%) in the sunitinib arm. The median OS was 47.2 months in the pembrolizumab plus axitinib arm and 40.8 months in the sunitinib arm (hazard ratio: 0.84; 95% confidence interval: 0.71–0.99) (Fig. 2a). Median PFS was 15.7 months in the pembrolizumab plus axitinib arm and 11.1 months in the sunitinib arm (hazard ratio: 0.69; 95% confidence interval: 0.59–0.81) (Fig. 2b). Consistent OS and PFS benefits with pembrolizumab plus

**Table 1 | Baseline characteristics in the intention-to-treat population**

	Pembrolizumab plus axitinib n=432	Sunitinib n=429
Age, median (range), years	62.0 (30–89)	61.0 (26–90)
<65 years	260 (60.2)	278 (64.8)
Sex		
Male	308 (71.3)	320 (74.6)
Female	124 (28.7)	109 (25.4)
Region of enrollment		
North America	104 (24.1)	103 (24.0)
Western Europe	106 (24.5)	104 (24.2)
Rest of the world	222 (51.4)	222 (51.7)
IMDC risk group		
Favorable	138 (31.9)	131 (30.5)
Intermediate	238 (55.1)	246 (57.3)
Poor	56 (13.0)	52 (12.1)
Sarcomatoid features		
Yes	51 (11.8)	54 (12.6)
No	234 (54.2)	239 (55.7)
Unknown or missing	147 (34.0)	136 (31.7)
PD-L1 CPS <sup>a</sup>		
≥1	243 (56.3)	254 (59.2)
<1	167 (38.7)	158 (36.8)
Missing or unknown	22 (5.1)	17 (4.0)
No. of organs with metastases		
1	114 (26.4)	96 (22.4)
≥2	315 (72.9)	331 (77.2)
Missing	3 (0.7)	2 (0.5)
Most common sites of metastasis		
Lung	312 (72.2)	309 (72.0)
Lymph node	199 (46.1)	197 (45.9)
Bone	103 (23.8)	103 (24.0)
Adrenal gland	67 (15.5)	76 (17.7)
Liver	66 (15.3)	71 (16.6)
Previous radiotherapy	41 (9.5)	40 (9.3)
Previous nephrectomy	357 (82.6)	358 (83.4)

Data are n (%) unless otherwise noted. <sup>a</sup>PD-L1 expression was centrally determined using the PD-L1 IHC 22C3 pharmDx (Agilent Technologies). CPS was calculated as the number of PD-L1-staining cells (tumor cells, lymphocytes and macrophages) divided by the total number of viable tumor cells, multiplied by 100.

axitinib compared to sunitinib were seen across subgroups, including International Metastatic Renal Cell Carcinoma Database Consortium (IMDC) risk favorable and intermediate-risk and poor-risk categories and PD-L1 combined positive score (CPS) cutoff values of <1 and ≥1 (Fig. 2c,d).

Confirmed ORR was 60.6% (50 complete responses (11.6%), 212 partial responses (49.1%)) in the pembrolizumab plus axitinib arm and 39.6% (17 complete responses (4.0%), 153 partial responses (35.7%)) in the sunitinib arm (Extended Data Table 1). The median duration of response (DOR) was 23.6 months (range, 1.4+ months to 68.6+ months) in the pembrolizumab plus axitinib arm and 15.3 months (range, 2.3–68.3 months) in the sunitinib arm (Fig. 2e). The estimated percentage of participants with an objective response who would have an ongoing

response at 60 months was 26.0% in the pembrolizumab plus axitinib arm and 14.4% in the sunitinib arm.

In a post hoc analysis of participants who completed 35 cycles of pembrolizumab (*n* = 120) (Supplementary Table 2), the median OS was not reached (95% confidence interval: 70.6 months to not reached), and the estimated 48-month and 60-month OS rates were 81.7% and 70.7%, respectively (Supplementary Fig. 1a). The median PFS was 37.4 months (95% confidence interval: 32.3–43.7 months), and the estimated 48-month and 60-month PFS rates were 38.3% and 32.8%, respectively (Supplementary Fig. 1b). The confirmed ORR was 85.0% (102/120; 22 complete responses (18.3%), 80 partial responses (66.7%)) (Supplementary Table 2).

### Biomarker outcomes

**Biomarker analysis population.** Of 848 RNA sequencing samples, 797 passed quality control, resulting in a 94.0% success rate. Of the 775 whole-exome sequencing (WES) tumor samples with matched normal samples, 751 passed quality control, resulting in a 96.9% success rate. Of the samples that passed quality control, duplicates and samples from participants who did not receive study treatment were further excluded from the biomarker analysis population. Of 854 participants who received at least one dose of study treatment in the total KEYNOTE-426 population, 730 (85.5%) had evaluable RNA sequencing data, 698 (81.7%) had evaluable WES data and 816 (95.6%) had evaluable PD-L1 CPS data (Supplementary Table 3). Baseline characteristics in the evaluable RNA sequencing and WES analyses populations were well balanced between treatment arms and similar to those of the total study population (Table 1 and Supplementary Table 3). Consistent with the intention-to-treat population, OS and PFS favored pembrolizumab plus axitinib over sunitinib in the RNA sequencing and WES analyses populations (Supplementary Table 3).

**Tcell<sub>inf</sub>GEP, angiogenesis signature and PD-L1 CPS.** Based on observed associations between biomarkers and clinical outcomes of pembrolizumab monotherapy in previous studies<sup>23–28</sup>, we examined whether an IFN $\gamma$ -related 18-gene Tcell<sub>inf</sub>GEP, the angiogenesis signature and PD-L1 CPS were separately associated with clinical outcomes of pembrolizumab plus axitinib or sunitinib. In the pembrolizumab plus axitinib arm, higher Tcell<sub>inf</sub>GEP was associated with improved ORR (*P* < 0.0001), PFS (*P* < 0.0001) and OS (*P* = 0.002) (Table 2). In the sunitinib arm, no associations (*P* > 0.05) were observed between Tcell<sub>inf</sub>GEP and clinical outcomes (Table 2 and Fig. 3a). For the angiogenesis signature, a positive association was observed only with OS (*P* = 0.004) in the pembrolizumab plus axitinib arm, and there was a positive association with ORR (*P* = 0.002), PFS (*P* < 0.001) and OS (*P* < 0.001) in the sunitinib arm (Table 2 and Fig. 3b). The significance of Tcell<sub>inf</sub>GEP to clinical outcomes in the pembrolizumab plus axitinib arm and the significance of angiogenesis to clinical outcomes in the sunitinib arm remained the same in the joint Tcell<sub>inf</sub>GEP and angiogenesis model (Supplementary Table 4). PD-L1 CPS as a continuous variable (square root scale) was negatively associated with OS for sunitinib (*P* = 0.025). No association was observed between continuous PD-L1 CPS and clinical outcomes for pembrolizumab plus axitinib (*P* > 0.05) (Table 2 and Fig. 3c), suggesting that PD-L1 expression (as measured by CPS) is not a predictive marker of outcomes with pembrolizumab plus axitinib in this disease setting. However, PD-L1 CPS showed a moderate correlation with Tcell<sub>inf</sub>GEP (Spearman  $\rho$  = 0.46) (Extended Data Fig. 1), supportive of the respective roles of PD-L1 expression and Tcell<sub>inf</sub>GEP in biologically defining an inflamed tumor microenvironment.

When assessing Tcell<sub>inf</sub>GEP using a prespecified cutoff of the first tertile, improved OS and PFS for pembrolizumab plus axitinib compared to sunitinib was observed in the Tcell<sub>inf</sub>GEP<sup>non-low</sup> subgroup (OS hazard ratio: 0.77 (95% confidence interval: 0.61–0.96); PFS hazard ratio: 0.58 (95% confidence interval: 0.47–0.72)) (Fig. 4a,b). When assessing angiogenesis signature using a cutoff of ≥ or < the median, PFS favored

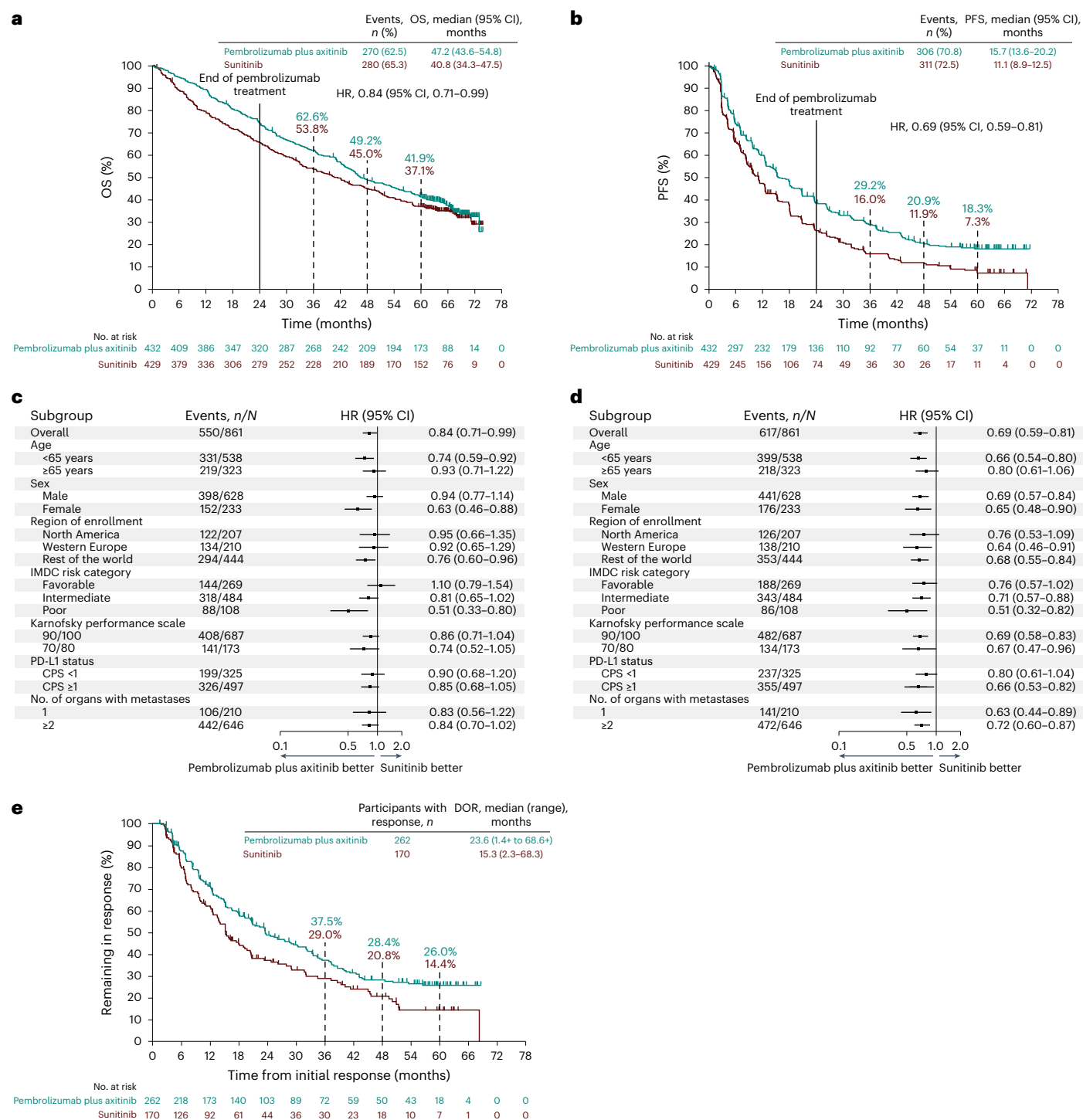


**Fig. 2 | OS, PFS and DOR in the intention-to-treat population. a**, Kaplan–Meier estimates of OS. **b**, Kaplan–Meier estimates of PFS. **c**, OS by subgroups. **d**, PFS by subgroups. **e**, Kaplan–Meier estimates of DOR in participants with a confirmed

objective response. In **a**, **b** and **e**, tick marks represent censored data. In **c** and **d**, shaded squares correspond to the hazard ratios (HRs), and the error bars (horizontal lines) correspond to the 95% confidence intervals (CIs).

pembrolizumab plus axitinib over sunitinib in the ≥ median subgroup (hazard ratio: 0.73 (95% confidence interval: 0.57–0.94)) (Fig. 4c,d). Notably, OS and PFS more strongly favored pembrolizumab plus axitinib over sunitinib in the < median subgroup (OS hazard ratio: 0.69 (95% confidence interval, 0.54–0.89); PFS hazard ratio: 0.62 (95% confidence interval: 0.48–0.79)) (Fig. 4c,d).

**Other gene expression signatures and molecular subtype.** We evaluated other gene expression signatures and their association with

clinical outcomes by hypothesis testing within each treatment arm. In the pembrolizumab plus axitinib arm, the monocytic myeloid-derived suppressor cell (mMDSC) signature was positively associated with ORR ( $P = 0.058$ ), PFS ( $P = 0.039$ ) and OS ( $P = 0.057$ ) (Table 2). In the sunitinib arm, the hypoxia signature was positively associated with ORR and OS ( $P = 0.071$  and  $P = 0.094$ , respectively); the MYC signature was negatively associated with PFS and OS ( $P = 0.017$  and  $P < 0.001$ , respectively); and the proliferation signature was negatively associated with OS ( $P < 0.001$ ). When evaluating the independence of the gene



**Table 2 | Within-arm association *P* values among gene expression signatures, PD-L1 CPS and molecular subtypes and clinical outcomes**

	Pembrolizumab plus axitinib			Sunitinib		
	ORR	PFS	OS	ORR	PFS	OS
Gene expression signatures <sup>a</sup>						
Tcell <sub>inf</sub> GEP	<b>2.03×10<sup>-6</sup>(+)</b>	<b>1.41×10<sup>-5</sup>(+)</b>	<b>0.002 (+)</b>	0.741	0.464	0.547
Angiogenesis	0.202	0.244	<b>0.004 (+)</b>	<b>0.002 (+)</b>	<b>5.66×10<sup>-4</sup>(+)</b>	<b>1.69×10<sup>-7</sup>(+)</b>
Glycolysis	0.995	0.972	0.931	0.711	0.934	0.136
gMDSC	0.995	0.972	0.185	0.711	0.936	0.136
Hypoxia	0.243	0.265	0.404	<b>0.071 (+)</b>	0.979	<b>0.094(+)</b>
mMDSC	<b>0.058 (+)</b>	<b>0.039 (+)</b>	<b>0.057 (+)</b>	0.711	0.936	0.136
MYC	0.995	0.972	0.404	0.711	<b>0.017 (-)</b>	<b>1.50×10<sup>-4</sup>(-)</b>
Proliferation	0.995	0.972	0.314	0.684	0.269	<b>5.33×10<sup>-4</sup>(-)</b>
RAS	0.995	0.972	0.931	0.711	0.979	0.506
Stroma/EMT/TGFβ	0.995	0.972	0.931	0.711	0.979	0.479
WNT	0.995	0.150	0.931	0.711	0.979	0.526
Molecular subtypes <sup>b</sup>	0.243	0.265	0.202	0.711	0.979	<b>0.010</b>
PD-L1 CPS <sup>c</sup>	0.053	0.168	0.544	0.558	0.331	<b>0.025 (-)</b>

Association was evaluated using a logistic regression model (ORR) and a Cox proportional hazards regression model (PFS and OS), with adjustment for IMDC risk category. Bolded *P* values for Tcell<sub>inf</sub>GEP, angiogenesis signature and PD-L1 CPS indicate nominal statistical significance ( $\alpha < 0.05$ ); bolded *P* values for other gene expression signatures and molecular subtype indicate multiplicity-adjusted (Hochberg step-up procedure; tested as one family of 10 hypotheses within each treatment arm) statistical significance ( $\alpha < 0.10$ ). A '+' or '-' indicates that the observed association is positive or negative, respectively. In the pembrolizumab plus axitinib arm, a positive association (one-tailed test) was hypothesized for Tcell<sub>inf</sub>GEP and PD-L1 CPS; negative associations (one-tailed test) were hypothesized for glycolysis, proliferation, RAS and stroma/EMT/TGFβ; and non-zero associations (two-tailed test) were hypothesized for the remaining gene expression signatures and molecular subtype. In the sunitinib arm, a positive association (one-tailed test) was hypothesized for angiogenesis signature; negative associations (one-tailed test) were hypothesized for gMDSC, glycolysis, MYC, proliferation and RAS; and non-zero associations (two-tailed test) were hypothesized for the remaining gene expression signatures, PD-L1 CPS and molecular subtype. <sup>a</sup>Included 369 participants in the pembrolizumab plus axitinib arm and 361 participants in the sunitinib arm. <sup>b</sup>Likelihood ratio test was performed for molecular subtype by comparing the full model (with molecular subtype) with the reduced model (without molecular subtype). The analysis population included 369 participants in the pembrolizumab plus axitinib arm and 361 participants in the sunitinib arm. <sup>c</sup>Association test for PD-L1 CPS was performed using the square root scale. The PD-L1 CPS analysis population included 407 participants in the pembrolizumab plus axitinib arm and 409 participants in the sunitinib arm.

signatures with the angiogenesis signature, the mMDSC signature was significantly associated with improved ORR ( $P = 0.006$ ), PFS ( $P = 0.002$ ) and OS ( $P = 0.004$ ) in the pembrolizumab plus axitinib arm (Supplementary Table 4). After adjusting for the angiogenesis signature in the sunitinib arm, the hypoxia signature was no longer significantly associated with any clinical outcome; the MYC signature was negatively associated with PFS ( $P = 0.039$ ) and OS ( $P = 0.016$ ); and the proliferation signature was negatively associated with OS ( $P = 0.043$ ). These associations were weaker compared to those without adjustment, which can be partially explained by the correlations among the signatures with the angiogenesis signature. Among all samples analyzed, there was a modest positive correlation ( $\rho = 0.31$ ) (Extended Data Fig. 1) between the hypoxia and angiogenesis signatures, whereas there was a modestly negative correlation for the MYC and proliferation signatures with the angiogenesis signature ( $\rho = 0.28$  and  $\rho = 0.35$ , respectively) (Extended Data Fig. 1).

Given that Tcell<sub>inf</sub>GEP was reported to be predictive of response to pembrolizumab monotherapy in other settings<sup>24,29</sup>, we adjusted these gene expression signatures for Tcell<sub>inf</sub>GEP (in addition to IMDC risk category) to elucidate their additional predictive value for the pembrolizumab and axitinib combination (although adjustment was performed in both treatment arms). After adjusting for Tcell<sub>inf</sub>GEP in the pembrolizumab plus axitinib arm, no associations between clinical outcomes and mMDSC signature were observed, and the proliferation signature was negatively associated with OS ( $P = 0.007$ ) (Extended Data Table 2). Notably, mMDSC was strongly positively correlated with Tcell<sub>inf</sub>GEP ( $\rho = 0.70$ ) (Extended Data Fig. 1). The associations for other gene expression signatures within the sunitinib arm remained similar after adjusting for Tcell<sub>inf</sub>GEP. The hypoxia signature was positively associated with ORR and OS ( $P = 0.065$  and  $P = 0.095$ , respectively); the MYC signature was negatively associated with PFS and OS ( $P = 0.019$  and

$P < 0.001$ , respectively); and the proliferation signature was negatively associated with OS ( $P < 0.001$ ).

We additionally sought to assign tumor samples to molecular subtypes according to the transcriptomically defined clustering in the phase 3 IMmotion151 trial<sup>8</sup>. We observed that 18.4% of the treated participants in the RNA sequencing population were angiogenic–stromal, 15.1% were angiogenic, 21.6% were immune–proliferative, 14.9% were proliferative and 14.9% were stromal–proliferative (Supplementary Table 5 and Extended Data Fig. 2a); 15.1% of participants in the total RNA sequencing population could not be assigned to one of these five subtypes and constituted a sixth 'other' subtype. Next, we evaluated the distribution of these molecular subtypes across IMDC risk categories and by PD-L1 status and observed enrichment of the immune–proliferative subtype in the IMDC intermediate-risk and poor-risk groups and in participants with tumors of PD-L1 CPS  $\geq 1$  (Extended Data Fig. 2b,c); the angiogenic–stromal subtype was enriched in participants with tumors of PD-L1 CPS  $< 1$ .

Testing of the association of molecular subtype and clinical outcomes showed an association with OS ( $P = 0.010$ ) in the sunitinib arm (Table 2). After prespecified adjustment for Tcell<sub>inf</sub>GEP and the angiogenesis signature, no significant associations with clinical outcomes were observed in the pembrolizumab plus axitinib and sunitinib arms ( $P > 0.10$ ) (Extended Data Table 2). Within the pembrolizumab plus axitinib arm, the ORR was lowest (50.0%) in the stromal–proliferative subtype and highest (75.6%) in the immune–proliferative subtype (Extended Data Fig. 3a). Within the sunitinib arm, the ORR was lowest (34.0%) in the proliferative subtype and highest (51.8%) in the angiogenic subtype.

**Efficacy estimates by DNA mutational status.** We examined the impact of mutations in genes with clinical relevance to RCC in other

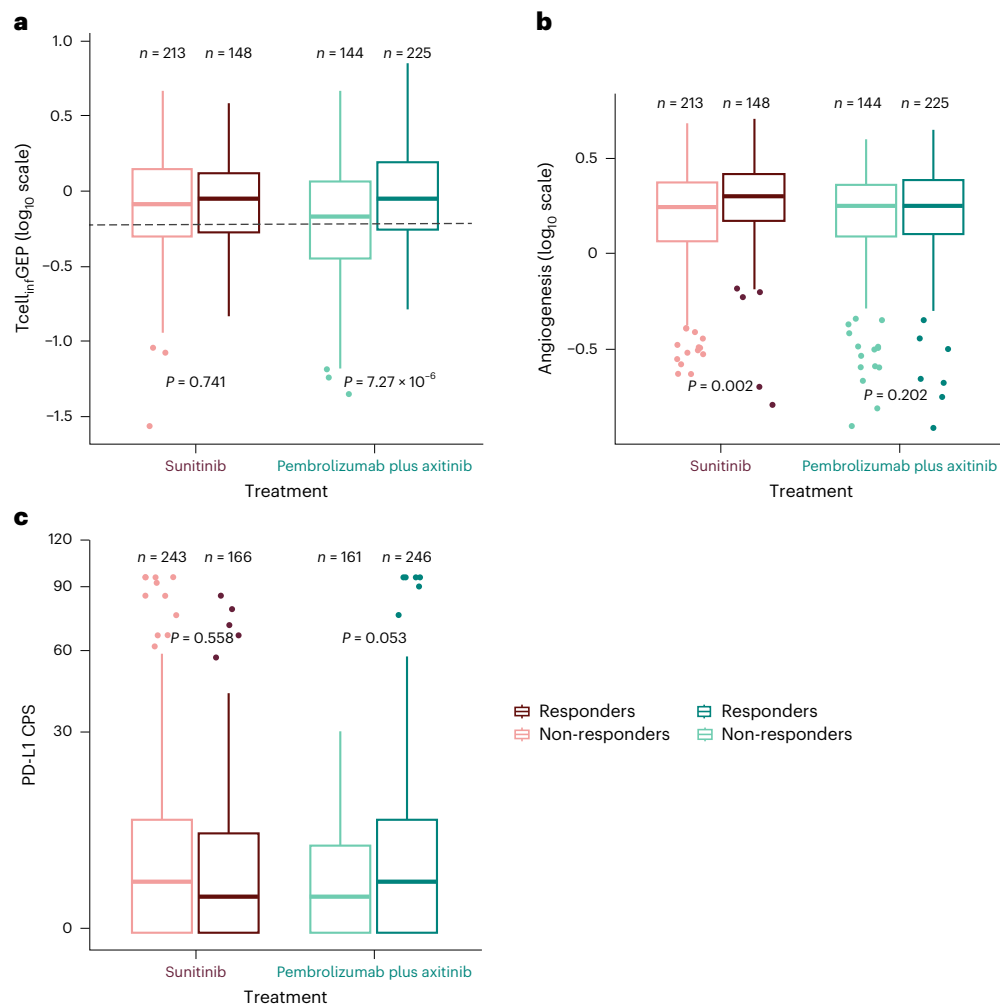


**Fig. 3 | Participant-level distribution of select biomarker scores by response status and treatment arm. a,** Tcell<sub>infl</sub>GEP (pembrolizumab plus axitinib,  $n = 369$ ; sunitinib,  $n = 361$ ). **b,** Angiogenesis signature (pembrolizumab plus axitinib,  $n = 369$ ; sunitinib,  $n = 361$ ). **c,** PD-L1 CPS (pembrolizumab plus axitinib,  $n = 407$ ; sunitinib,  $n = 409$ ). The center line corresponds to the median, and the box is delineated by the first and third quartiles. Whiskers extend to any points within

1.5 times the interquartile range, with points lying beyond identified individually as potential outliers.  $P$  values are nominal (one-sided for pembrolizumab plus axitinib and two-sided for sunitinib) and were derived using a logistic regression model, with adjustment for IMDC risk category. Significance was prespecified at  $\alpha = 0.05$ .

studies, including *VHL*, *SETD2* (SET domain containing 2, histone lysine methyltransferase), *PBRM1* and *BAP1* using WES<sup>8,14,30</sup>. In the pembrolizumab plus axitinib arm, no significant associations between DNA mutations and PFS or OS were observed (Extended Data Table 3). The *PBRM1* mutation was positively associated with the ORR within the pembrolizumab plus axitinib arm, with significantly higher rates in the *PBRM1* mutant than in the wild-type subgroup (71.4% versus 52.3%;  $P = 0.002$ ) (Extended Data Table 3 and Extended Data Fig. 3b). The ORR with the pembrolizumab plus axitinib was similar between the mutant and the wild-type subgroups for *VHL*, *SETD2* and *BAP1* (Extended Data Fig. 3b). In the sunitinib arm, *VHL* and *PBRM1* mutations were associated with longer OS ( $P = 0.040$  and  $P = 0.010$ , respectively), whereas *BAP1* mutation was associated with shorter OS ( $P = 0.019$ ) (Extended Data Table 3). The *VHL*, *PBRM1* and *SETD2* mutations were not associated with PFS or ORR in the sunitinib arm ( $P > 0.10$ ). The ORR with sunitinib was similar between the mutant and the wild-type subgroups for *VHL*, *PBRM1*, *SETD2* and *BAP1* (Extended Data Fig. 3c).

When assessing efficacy by DNA mutational status, OS and PFS directionally favored pembrolizumab plus axitinib over sunitinib, with various hazard ratios in the mutant and wild-type subgroups for *VHL*, *PBRM1*, *SETD2* and *BAP1* (Extended Data Figs. 4–7).

## Discussion

The final clinical follow-up analysis of KEYNOTE-426 showed sustained and durable clinical benefit of pembrolizumab plus axitinib compared to sunitinib<sup>2,31,32</sup>. In the prespecified exploratory biomarker analysis, significant associations between several genomic features and clinical outcomes with pembrolizumab plus axitinib or sunitinib were observed, which deepens understanding of RCC biology and potentially informs further advancement in treating patients with advanced clear cell RCC.

Higher Tcell<sub>infl</sub>GEP was associated with improved ORR, PFS and OS for pembrolizumab plus axitinib, but there was no association with clinical outcomes for sunitinib. This association with pembrolizumab plus axitinib was not unexpected given that the Tcell<sub>infl</sub>GEP comprises genes related to antigen presentation, adaptive immune resistance, cytolytic activity and chemokine expression<sup>23,29</sup>. The positive association between Tcell<sub>infl</sub>GEP and outcomes in the combination arm is consistent with previous reports for pembrolizumab monotherapy in the pan-tumor and specific tumor settings, including clear cell RCC managed with pembrolizumab monotherapy (KEYNOTE-427 cohort A) and with reports that showed associations between T cell inflammation-related genes and clinical outcomes for avelumab plus axitinib (JAVELIN Renal 101 trial) and atezolizumab

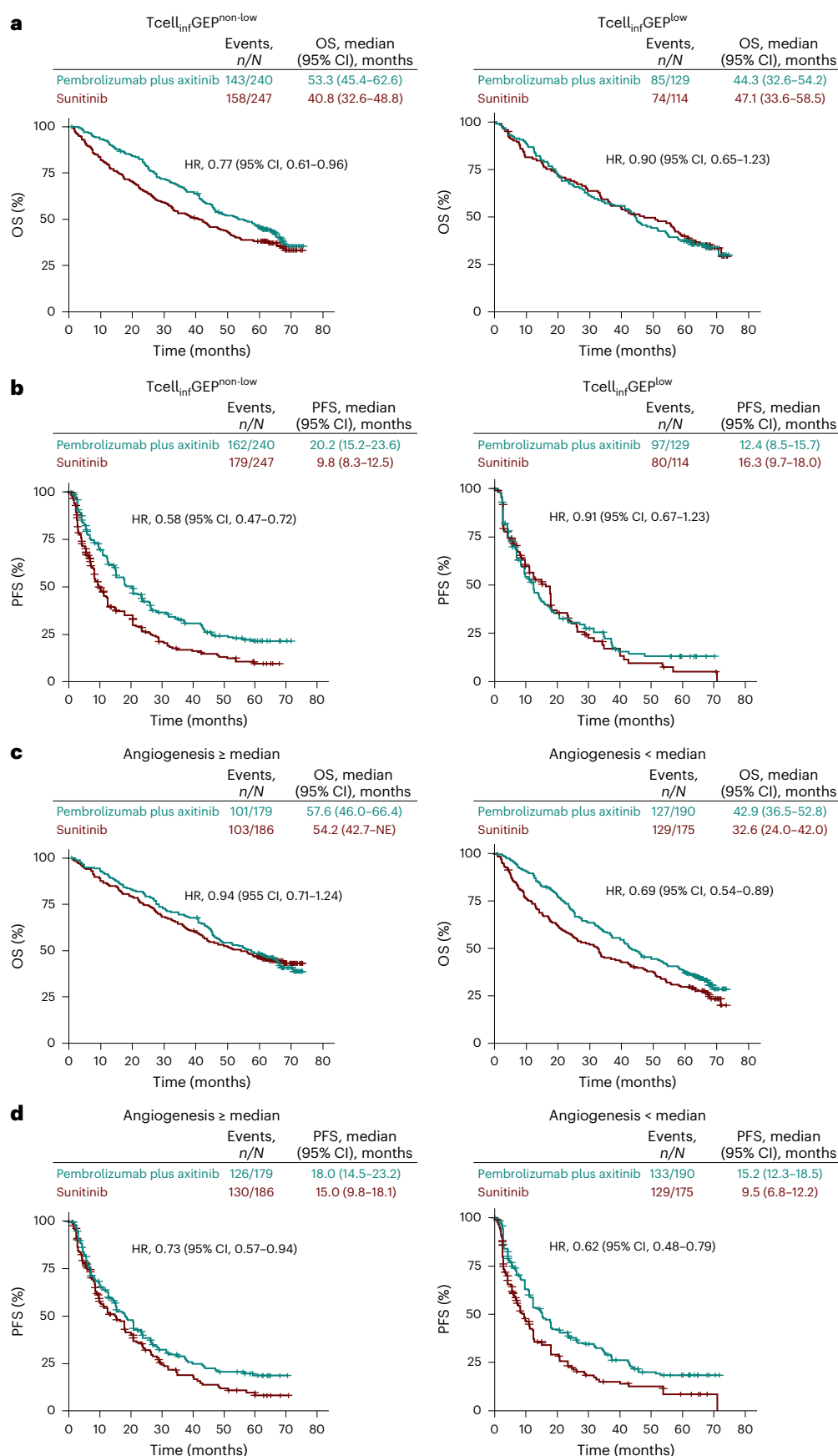


**Fig. 4 | Kaplan–Meier estimates of survival by Tcell<sub>inf</sub>GEP or angiogenesis signature cutoff. a, OS by Tcell<sub>inf</sub>GEP cutoff. b, PFS by Tcell<sub>inf</sub>GEP cutoff. c, OS by angiogenesis signature cutoff. d, PFS by angiogenesis signature cutoff. Tick marks represent censored data. CI, confidence interval; HR, hazard ratio.**

plus bevacizumab (IMmotion150/151 trial)<sup>23–29</sup>. However, in the phase 3 CLEAR/KEYNOTE-581 trial of participants with advanced clear cell RCC, Tcell<sub>inf</sub>GEP was not associated with ORR and PFS for lenvatinib plus pembrolizumab but was associated with ORR for sunitinib<sup>33</sup>. In the phase 3 CheckMate 9ER trial of participants with advanced clear cell RCC, several gene expression signatures, including IFN $\gamma$ , were not predictive of clinical outcomes of nivolumab plus cabozantinib<sup>19</sup>. The precise reasons for differences among the associations of immune signatures and outcomes across trials are not entirely clear but could include differences in the TKI partner, the number of evaluable samples and the duration of follow-up. The strength of the association between Tcell<sub>inf</sub>GEP and response seems to be greater with the pembrolizumab and axitinib combination than with pembrolizumab monotherapy in specific tumor types (including clear cell RCC in the KEYNOTE-427 trial)<sup>23,25,27–29</sup>, suggesting a potential positive interaction between the TKI and the PD-1 inhibitor. Preclinical models have shown that TKIs exert immune-modulatory effects in the tumor microenvironment by enhancing tumor cell sensitivity to immune-cell-mediated lysis through an alteration in the tumor cell phenotype and by altering the frequency or function of immune cell subsets in the periphery or the tumor microenvironment, thus promoting more productive immune interactions<sup>34–36</sup>. The hypothesis of a positive interaction between axitinib and pembrolizumab is further supported by the lack of significant associations between Tcell<sub>inf</sub>GEP and clinical outcomes for sunitinib, which suggests that the Tcell<sub>inf</sub>GEP is not a predictor of response to sunitinib as monotherapy. However, axitinib and sunitinib are different TKIs.

The strong positive association between angiogenesis signature and all clinical outcomes for sunitinib is consistent with previous reports from the phase 3 COMPARZ (first-line pazopanib versus sunitinib) and IMmotion151 (first-line atezolizumab plus bevacizumab versus sunitinib) studies of participants with advanced clear cell RCC, supporting the present findings<sup>8,10,14</sup>. Because TKI monotherapy is not commonly used as first-line therapy, these findings have limited clinical applicability. Whether this association would be seen in a refractory setting in which TKIs are commonly used requires further investigation.

Previous analyses of the IMmotion151 trial identified seven molecular clusters related to differential clinical outcomes with first-line atezolizumab plus bevacizumab compared to sunitinib across molecular subtypes<sup>8,10</sup>. Survival outcomes were poorer for participants with tumors classified within the angiogenic cluster who were given atezolizumab plus bevacizumab than for those given sunitinib (OS hazard ratio: 1.32)<sup>10</sup>. In the present analysis, results of assessment of the associations within arms showed a positive association of the angiogenesis signature with OS, and the OS hazard ratio for pembrolizumab plus axitinib compared to sunitinib in the high ( $\geq$  median) angiogenesis subgroup was 0.94. An understanding of the different antiangiogenic effects among different TKIs and between TKIs and bevacizumab as related to the association with an angiogenic gene signature requires further investigation. In the phase 3 JAVELIN Renal 101 trial, participants with advanced or metastatic RCC in clusters 1 (angiogenic–stromal), 3 (complement–oxidation) and 4 (T-effector–proliferative) treated with avelumab plus axitinib tended to have improved PFS compared to sunitinib-treated participants<sup>11</sup>. In the present analysis of the KEYNOTE-426 trial, the highest ORR for pembrolizumab plus axitinib was observed in the immune–proliferative cluster, as expected given that this cluster comprises tumors that are angiogenesis poor but highly immunogenic, with highest infiltration in immune cell subsets (CD8<sup>+</sup>, CD4<sup>+</sup> and regulatory T cells, B cells, macrophages and dendritic cells)<sup>8,10</sup>.

Genomic features, such as loss-of-function mutations in *VHL*, *PBRM1*, *SETD2* and *BAP1*, have been evaluated to determine their association with clinical outcomes of systemic therapies in patients with advanced clear cell RCC; however, data are often conflicting<sup>8,12–18,30</sup>. The relationship between clinical outcomes and *PBRM1* DNA alterations has attracted attention in the past. Although the present dataset

showed that *PBRM1* mutation tended to be associated with improved outcomes, *PBRM1* mutation does not seem to be a reliable biomarker considering the totality of the data.

Although PD-L1 CPS has been positively associated with clinical outcomes of pembrolizumab monotherapy or pembrolizumab-based combination treatment in advanced clear cell RCC and other tumor types<sup>25,28</sup>, the lack of a significant association between PD-L1 CPS and clinical outcomes in the present analyses suggests that PD-L1 expression (as measured by CPS) is not a predictive marker of outcomes of pembrolizumab plus axitinib in this disease setting and should not be used in this clinical setting. Similarly, PD-L1 expression (tumor proportion score  $\geq 1\%$ ) was not associated with clinical outcomes of nivolumab plus cabozantinib in the CheckMate 9ER trial<sup>19</sup>. Notably, Tcell<sub>inf</sub>GEP, which was positively associated with clinical outcomes within the pembrolizumab plus axitinib arm, was moderately correlated with PD-L1 CPS (this correlation is not unexpected given that the Tcell<sub>inf</sub>GEP includes mRNA expressions for PD-L1)<sup>29</sup>. These data suggest the respective roles of Tcell<sub>inf</sub>GEP and PD-L1 CPS in biologically defining an inflamed tumor microenvironment, but their independent contribution as predictive biomarkers of immunotherapy may be therapy specific and tumor type specific<sup>24,26,29</sup>.

These data have both clinical and biomarker relevance in the treatment choice for patients with advanced clear cell RCC. First, with longer follow-up of patients in the KEYNOTE-426 trial and other phase 3 trials of a VEGF-TKI plus PD-1 inhibitor (CheckMate 9ER (cabozantinib plus nivolumab) and CLEAR/KEYNOTE-581 (lenvatinib plus pembrolizumab)), as well as more mature data for the cytotoxic T-lymphocyte-associated protein 4 (CTLA-4) inhibitor ipilimumab plus nivolumab (CheckMate 214), all four treatment approaches remain reasonable, supported by a significant survival advantage<sup>37–39</sup>. Second, employing the IMDC risk score to select therapy appears increasingly flawed; it remains a useful prognostic tool based on clinical characteristics rather than tissue-based biomarkers. Biomarker data from this and previous trials show some consistency but also many instances of inconsistency<sup>8–11,14,19,20</sup>. Although the signatures evaluated in this trial look promising, particularly for sunitinib, and other studies have shown potential clinical utility of molecular subsets and emerging biomarkers (for example, serum glycopeptides and circulating KIM-1)<sup>8,10,11,20–22</sup>, it is not currently possible to define a biomarker to select for combination regimens with either a specific VEGF-TKI plus PD-1 inhibitor or CTLA-4 inhibitor plus PD-1 inhibitor. Moving forward, prospective biomarker trials are ongoing, including those testing for PD-L1 expression and RNA signatures<sup>30,40,41</sup>.

A strength of the biomarker analysis is that the populations included a high proportion of the treated population in each arm; therefore, inferences drawn from these respective datasets are largely representative of the KEYNOTE-426 trial population. However, the prespecified exploratory biomarker analysis from the KEYNOTE-426 trial is limited by the small sample sizes of some of the subgroups and the lack of statistical power and (or) multiplicity adjustments for association analysis of some biomarkers, hindering definitive conclusions. Additionally, given the complex interplay of biological processes involved in the RCC tumor microenvironment<sup>42</sup>, the evaluation of each signature or gene individually most likely does not capture the potential joint effects of the biomarkers on clinical outcomes within each treatment arm. Furthermore, inter-trial differences in definitions for PD-L1 expression, different algorithms for clustering patient samples into molecular subtypes and different gene expression signatures evaluated limit comparative interpretations of the biomarker data. Lastly, because a VEGF-TKI was present in both treatment arms, the relative contribution of VEGF-TKI in the survival outcomes cannot be determined from a clinical and biomarker standpoint.

In conclusion, results of the present analysis showed sustained OS, PFS and ORR benefit of the use of pembrolizumab plus axitinib compared to sunitinib monotherapy. An extensive biomarker analysis



adds to the increasing amount of information on biomarkers in patients treated with immunotherapy-based combinations. Although the analysis showed potential clinical utility of some RNA signatures in identifying patients who are likely to benefit the most from each treatment, additional correlative data and further prospective clinical investigations are needed to inform biomarker-directed treatment of patients with advanced or metastatic RCC who are being considered for combination treatment with antiangiogenic and PD-1 inhibitor therapies. Pembrolizumab plus axitinib is a first-line treatment option for patients with advanced RCC regardless of biomarker subtypes.

## Online content

Any methods, additional references, Nature Portfolio reporting summaries, source data, extended data, supplementary information, acknowledgements, peer review information; details of author contributions and competing interests; and statements of data and code availability are available at <https://doi.org/10.1038/s41591-025-03867-5>.

## References

1. Keytruda (pembrolizumab injection), for intravenous use. Package insert. (Merck & Co., Inc., 2025).
2. Rini, B. I. et al. Pembrolizumab plus axitinib versus sunitinib for advanced renal-cell carcinoma. *N. Engl. J. Med.* **380**, 1116–1127 (2019).
3. Ljungberg, B. et al. EAU guidelines on renal cell carcinoma. European Association of Urology <https://d56bochlqxzn.cloudfront.net/documents/full-guideline/EAU-Guidelines-on-Renal-Cell-Carcinoma-2023.pdf> (2023).
4. Motzer, R. J. et al. NCCN Guidelines® Insights: Kidney Cancer, Version 2.2024. *J. Natl Compr. Cancer Netw.* **22**, 4–16 (2024).
5. Powles, T. et al. Renal cell carcinoma: ESMO clinical practice guideline for diagnosis, treatment and follow-up. *Ann. Oncol.* **35**, 692–706 (2024).
6. Raimondi, A. et al. Predictive biomarkers of response to immunotherapy in metastatic renal cell cancer. *Front. Oncol.* **10**, 1644 (2020).
7. Lyskjær, I. et al. Management of renal cell carcinoma: promising biomarkers and the challenges to reach the clinic. *Clin. Cancer Res.* **30**, 663–672 (2024).
8. Motzer, R. J. et al. Molecular subsets in renal cancer determine outcome to checkpoint and angiogenesis blockade. *Cancer Cell* **38**, 803–817 (2020).
9. Motzer, R. J. et al. Avelumab plus axitinib versus sunitinib in advanced renal cell carcinoma: biomarker analysis of the phase 3 JAVELIN Renal 101 trial. *Nat. Med.* **26**, 1733–1741 (2020).
10. Motzer, R. J. et al. Final overall survival and molecular analysis in IMmotion151, a phase 3 trial comparing atezolizumab plus bevacizumab vs sunitinib in patients with previously untreated metastatic renal cell carcinoma. *JAMA Oncol.* **8**, 275–280 (2022).
11. Saliby, R. M. et al. Impact of renal cell carcinoma molecular subtypes on immunotherapy and targeted therapy outcomes. *Cancer Cell* **42**, 732–735 (2024).
12. Signoretti, S. et al. Renal cell carcinoma in the era of precision medicine: from molecular pathology to tissue-based biomarkers. *J. Clin. Oncol.* **36**, JCO2018792259 (2018).
13. Hakimi, A. A. et al. A pan-cancer analysis of PBAF complex mutations and their association with immunotherapy response. *Nat. Commun.* **11**, 4168 (2020).
14. Hakimi, A. A. et al. Transcriptomic profiling of the tumor microenvironment reveals distinct subgroups of clear cell renal cell cancer: data from a randomized phase III trial. *Cancer Discov.* **9**, 510–525 (2019).
15. McDermott, D. F. et al. Clinical activity and molecular correlates of response to atezolizumab alone or in combination with bevacizumab versus sunitinib in renal cell carcinoma. *Nat. Med.* **24**, 749–757 (2018).
16. Miao, D. et al. Genomic correlates of response to immune checkpoint therapies in clear cell renal cell carcinoma. *Science* **359**, 801–806 (2018).
17. Santos, M. et al. *PBRM1* and *KDM5C* cooperate to define high-angiogenesis tumors and increased antiangiogenic response in renal cancer. *Am. J. Cancer Res.* **13**, 2116–2125 (2023).
18. Braun, D. A. et al. Clinical validation of *PBRM1* alterations as a marker of immune checkpoint inhibitor response in renal cell carcinoma. *JAMA Oncol.* **5**, 1631–1633 (2019).
19. Choueiri, T. K. et al. Biomarker analysis from the phase 3 CheckMate 9ER trial of nivolumab + cabozantinib v sunitinib for advanced renal cell carcinoma (aRCC). *J. Clin. Oncol.* **41**, 608 (2023).
20. Braun, D. A. et al. 1694MO Novel serum glycoproteomic biomarkers predict response to nivolumab plus cabozantinib (NIVO+CABO) versus sunitinib (SUN) in advanced RCC (aRCC): analysis from CheckMate 9ER. *Ann. Oncol.* **35**, S1012–S1013 (2024).
21. Machaalani, M. et al. KIM-1 as a circulating biomarker in metastatic RCC: post-hoc analysis of JAVELIN Renal 101. *J. Clin. Oncol.* **43**, 594 (2025).
22. Xu, W. et al. Evaluation of circulating kidney injury marker-1 (KIM-1) as a prognostic and predictive biomarker in advanced renal cell carcinoma (aRCC): post-hoc analysis of CheckMate 214. *J. Clin. Oncol.* **43**, 437 (2025).
23. Cristescu, R. et al. Pan-tumor genomic biomarkers for PD-1 checkpoint blockade-based immunotherapy. *Science* **362**, eaar3593 (2018).
24. Cristescu, R. et al. Transcriptomic determinants of response to pembrolizumab monotherapy across solid tumor types. *Clin. Cancer Res.* **28**, 1680–1689 (2022).
25. Bellmunt, J. et al. Putative biomarkers of clinical benefit with pembrolizumab in advanced urothelial cancer: results from the KEYNOTE-045 and KEYNOTE-052 landmark trials. *Clin. Cancer Res.* **28**, 2050–2060 (2022).
26. Ott, P. A. et al. T-cell-inflamed gene-expression profile, programmed death ligand 1 expression, and tumor mutational burden predict efficacy in patients treated with pembrolizumab across 20 cancers: KEYNOTE-028. *J. Clin. Oncol.* **37**, 318–327 (2019).
27. Shitara, K. et al. Association between gene expression signatures and clinical outcomes of pembrolizumab versus paclitaxel in advanced gastric cancer: exploratory analysis from the randomized, controlled, phase III KEYNOTE-061 trial. *J. Immunother. Cancer* **11**, e006920 (2023).
28. McDermott, D. F. et al. Association of gene expression with clinical outcomes in patients with renal cell carcinoma treated with pembrolizumab in KEYNOTE-427. *J. Clin. Oncol.* **38**, 5024 (2020).
29. Ayers, M. et al. IFN- $\gamma$ -related mRNA profile predicts clinical response to PD-1 blockade. *J. Clin. Invest.* **127**, 2930–2940 (2017).
30. Saliby, R. M. et al. Update on biomarkers in renal cell carcinoma. *Am. Soc. Clin. Oncol. Educ. Book* **44**, e430734 (2024).
31. Powles, T. et al. Pembrolizumab plus axitinib versus sunitinib monotherapy as first-line treatment of advanced renal cell carcinoma (KEYNOTE-426): extended follow-up from a randomised, open-label, phase 3 trial. *Lancet Oncol.* **21**, 1563–1573 (2020).
32. Plimack, E. R. et al. Pembrolizumab plus axitinib versus sunitinib as first-line treatment of advanced renal cell carcinoma: 43-month follow-up of the phase 3 KEYNOTE-426 study. *Eur. Urol.* **84**, 449–454 (2023).
33. Motzer, R. J. et al. Biomarker analyses from the phase III randomized CLEAR trial: lenvatinib plus pembrolizumab versus sunitinib in advanced renal cell carcinoma. *Ann. Oncol.* **36**, 375–386 (2024).

34. Lu, C. et al. Understanding the dynamics of TKI-induced changes in the tumor immune microenvironment for improved therapeutic effect. *J. Immunother. Cancer* **12**, e009165 (2024).
35. Nuti, M. et al. Immunomodulatory effects of tyrosine kinase inhibitors (TKIs) in renal cell carcinoma (RCC) patients. *J. Clin. Oncol.* **35**, e14506 (2017).
36. Aparicio, L. M. A. et al. Tyrosine kinase inhibitors reprogramming immunity in renal cell carcinoma: rethinking cancer immunotherapy. *Clin. Transl. Oncol.* **19**, 1175–1182 (2017).
37. Motzer, R. J. et al. Lenvatinib plus pembrolizumab versus sunitinib in first-line treatment of advanced renal cell carcinoma: final prespecified overall survival analysis of CLEAR, a phase III study. *J. Clin. Oncol.* **42**, 1222–1228 (2024).
38. Tannir, N. M. et al. Nivolumab plus ipilimumab versus sunitinib for first-line treatment of advanced renal cell carcinoma: extended 8-year follow-up results of efficacy and safety from the phase 3 CheckMate 214 trial. *Ann. Oncol.* **35**, 1026–1038 (2024).
39. Motzer, R. J. et al. Nivolumab plus cabozantinib (N+C) vs sunitinib (S) for previously untreated advanced renal cell carcinoma (aRCC): final follow-up results from the CheckMate 9ER trial. *J. Clin. Oncol.* **43**, 439 (2025).
40. Reddy, A. et al. Biomarker-driven prospective clinical trial in renal cell carcinoma: developing machine learning models to allocate patients to treatment arms using RNA sequencing. *J. Clin. Oncol.* **41**, 4525 (2023).
41. Chouieri, T. SAMETA: a phase III study of savolitinib + durvalumab vs sunitinib and durvalumab monotherapy in patients with MET-driven, unresectable, locally advanced/metastatic papillary renal cell carcinoma. *Oncologist* **28**, S11–S12 (2023).
42. Monjaras-Avila, C. U. et al. The tumor immune microenvironment in clear cell renal cell carcinoma. *Int. J. Mol. Sci.* **24**, 7946 (2023).

**Publisher's note** Springer Nature remains neutral with regard to jurisdictional claims in published maps and institutional affiliations.

**Open Access** This article is licensed under a Creative Commons Attribution 4.0 International License, which permits use, sharing, adaptation, distribution and reproduction in any medium or format, as long as you give appropriate credit to the original author(s) and the source, provide a link to the Creative Commons licence, and indicate if changes were made. The images or other third party material in this article are included in the article's Creative Commons licence, unless indicated otherwise in a credit line to the material. If material is not included in the article's Creative Commons licence and your intended use is not permitted by statutory regulation or exceeds the permitted use, you will need to obtain permission directly from the copyright holder. To view a copy of this licence, visit <http://creativecommons.org/licenses/by/4.0/>.

© The Author(s) 2025

**Brian I. Rini** <sup>1</sup>✉, **Elizabeth R. Plimack** <sup>2</sup>, **Viktor Stus** <sup>3</sup>, **Rustem Gafanov**<sup>4</sup>, **Tom Waddell** <sup>5</sup>, **Dmitry Nosov**<sup>6</sup>, **Frédéric Pouliot**<sup>7</sup>, **Boris Alekseev**<sup>8</sup>, **Denis Soulières** <sup>9</sup>, **Bohuslav Melichar**<sup>10</sup>, **Ihor Vynnychenko**<sup>11</sup>, **Sergio Jobim de Azevedo**<sup>12</sup>, **Delphine Borchellini**<sup>13</sup>, **Raymond S. McDermott** <sup>14</sup>, **Jens Bedke**<sup>15</sup>, **Satoshi Tamada**<sup>16</sup>, **Sterling Wu**<sup>17</sup>, **Julia Markensohn**<sup>17</sup>, **Yiwei Zhang**<sup>17</sup>, **Andrey Loboda** <sup>17</sup>, **Amir Vajdi** <sup>17</sup>, **Rodolfo F. Perini**<sup>17</sup>, **Joseph Burgents**<sup>17</sup> & **Thomas Powles** <sup>18</sup>

<sup>1</sup>Vanderbilt-Ingram Cancer Center, Nashville, TN, USA. <sup>2</sup>Fox Chase Cancer Center, Philadelphia, PA, USA. <sup>3</sup>Dnipro State Medical University, Dnipro, Ukraine. <sup>4</sup>Russian Scientific Center of Roentgenoradiology, Moscow, Russia. <sup>5</sup>The Christie NHS Foundation Trust, Manchester, UK. <sup>6</sup>Central Clinical Hospital With Outpatient Clinic, Moscow, Russia. <sup>7</sup>CHU of Québec and Laval University, Quebec, Quebec, Canada. <sup>8</sup>P. Herzen Moscow Oncology Research Institute, Ministry of Health of the Russian Federation, Moscow, Russia. <sup>9</sup>Centre Hospitalier de l'Université de Montréal, Montreal, Quebec, Canada. <sup>10</sup>Palacký University Medical School and Teaching Hospital, Olomouc, Czech Republic. <sup>11</sup>Sumy State University, Sumy Regional Oncology Center, Sumy, Ukraine. <sup>12</sup>Hospital de Clínicas de Porto Alegre, Porto Alegre, Brazil. <sup>13</sup>Centre Antoine Lacassagne, Université Côte d'Azur, Nice, France. <sup>14</sup>St. Vincent's University Hospital and University College Dublin, Dublin, Ireland. <sup>15</sup>Department of Urology and Transplantation Surgery, Eva Mayr-Stihl Cancer Center, Klinikum Stuttgart, Stuttgart, Germany. <sup>16</sup>Bell-Land General Hospital, Osaka, Japan. <sup>17</sup>Merck & Co., Inc., Rahway, NJ, USA. <sup>18</sup>Barts Health Biomedical Research Center, Queen Mary's University of London ECMC, London, UK. ✉e-mail: [brian.rini@vumc.org](mailto:brian.rini@vumc.org)

## Methods

### Inclusion and ethics

KEYNOTE-426 (NCT02853331) is a randomized, open-label, phase 3 trial conducted across 129 medical centers globally. The trial was conducted in accordance with the principles of Good Clinical Practice and was approved by the appropriate institutional review boards and regulatory agencies. Written informed consent was provided by all participants before enrollment.

### Trial design, participants and treatments

Details of the trial design and eligibility criteria were published previously<sup>2,31</sup>. In brief, eligible participants were adults with newly diagnosed stage IV or recurrent clear cell RCC who had not previously received systemic therapy for advanced disease. Participants had a Karnofsky Performance Scale score of 70% or higher at baseline, one or more measurable lesions per Response Evaluation Criteria in Solid Tumors version 1.1 (RECIST v1.1) as assessed by the investigator and a tumor sample available for biomarker assessment. Sex of participants was determined based on self-report.

Participants were randomly assigned in a 1:1 ratio to receive pembrolizumab 200 mg intravenously once every 3 weeks for up to 35 cycles (~2 years) plus axitinib 5 mg by mouth twice daily continuously or sunitinib 50 mg by mouth once daily for 4 weeks on and 2 weeks off, continuously. Randomization was stratified according to the IMDC risk group (favorable versus intermediate versus poor risk) and by geographic region (North America versus Western Europe versus rest of the world). Treatment was continued until disease progression, unacceptable toxicity or physician or participant decision to discontinue. In the pembrolizumab plus axitinib arm, if one drug was discontinued because of toxicity, the other drug could be continued.

### Outcomes

The dual primary endpoints of OS and PFS per RECIST v1.1 by blinded independent central review (BICR) and key secondary endpoint of ORR per RECIST v1.1 by BICR were met at the first interim analysis<sup>2</sup>. Therefore, the subsequent analyses of efficacy are exploratory.

The prespecified objectives of the exploratory biomarker analysis, defined in a statistical analysis plan, were as follows:

- (1) To assess whether an IFN $\gamma$ -related 18-gene Tcell<sub>inf</sub>GEP and 10 other signatures (angiogenesis, glycolysis, granulocytic myeloid-derived suppressor cells (gMDSCs), hypoxia, mMDSCs, MYC, proliferation, RAS, stroma/EMT/TGF $\beta$  and WNT)<sup>24</sup> are individually associated with clinical outcomes (ORR, OS and PFS) of pembrolizumab plus axitinib or sunitinib;
- (2) To assess whether prespecified molecular subtypes as categorical variables are separately associated with clinical outcomes of pembrolizumab plus axitinib or of sunitinib;
- (3) To assess whether continuous PD-L1 CPS is separately associated with clinical outcomes of pembrolizumab plus axitinib or of sunitinib; and
- (4) To assess whether mutation status of key RCC driver genes (*VHL*, *PBRM1*, *SETD2* and *BAP1*), as determined by WES, are separately associated with clinical outcomes of pembrolizumab plus axitinib or of sunitinib.

Estimation of PFS and OS hazard ratios for pembrolizumab plus axitinib compared to sunitinib was also performed by Tcell<sub>inf</sub>GEP subgroups based on a prespecified cutoff of the first tertile<sup>23</sup>; by angiogenesis signature subgroups defined by a prespecified cutoff of the median; and by mutational status of *VHL*, *PBRM1*, *SETD2* and *BAP1*.

### Assessments

Details on the assessment of efficacy outcomes were published previously and follow standard guidance by the US Food and

Drug Administration (<https://www.fda.gov/regulatory-information/search-fda-guidance-documents/clinical-trial-endpoints-approval-cancer-drugs-and-biologics>)<sup>2,31,43</sup>. For the biomarker analysis, formalin-fixed, paraffin-embedded (FFPE) pretreatment tumor tissue samples collected at screening were used. PD-L1 expression was centrally determined using the PD-L1 IHC 22C3 pharmDx (Agilent Technologies). CPS was calculated as the number of PD-L1-staining cells (tumor cells, lymphocytes and macrophages) divided by the total number of viable tumor cells, multiplied by 100.

RNA sequencing was performed on an Illumina HiSeq by use of the TruSeq Access protocol. Raw reads were processed using a customized data analysis pipeline in OmicSoft Array Suite version 9 (Qiagen)<sup>24</sup>. In brief, the raw sequence reads were filtered for quality and subsequently aligned to the reference genome Human.B37.3 using OmicSoft Sequence Aligner<sup>44</sup>. After reference alignment, gene expression levels (raw read counts and fragments per kilobase of exon per million mapped fragments) were quantified using the RNA-Seq by Expectation Maximization (RSEM) algorithm<sup>45</sup> with the gene model Ensembl.R75. The Tcell<sub>inf</sub>GEP is composed of 18 inflammatory genes related to antigen presentation, adaptive immune resistance, cytolytic activity and chemokine expression, including *CCL5*, *CD27*, *CD274* (PD-L1), *CD276* (B7-H3), *CD8A*, *CMKLR1*, *CXCL9*, *CXCR6*, *HLA-DQA1*, *HLA-DRB1*, *HLA-E*, *IDO1*, *LAG3*, *NRG7*, *PDCD1LG2* (PD-L2), *PSMB10*, *STAT1* and *TIGIT*<sup>23,29</sup>. The Tcell<sub>inf</sub>GEP score was calculated as the weighted sum of normalized expression values for the 18 genes. The Tcell<sub>inf</sub>GEP was established on the NanoString platform (NanoString Technologies), was evaluated across the pembrolizumab clinical development program and was predictive of response to pembrolizumab in both pan-tumor and histology-specific settings<sup>23–25,27–29</sup>. The 10 other signature scores (angiogenesis, glycolysis, gMDSCs, hypoxia, mMDSCs, MYC, proliferation, RAS, stroma/EMT/TGF $\beta$  and WNT) were calculated as the average of the genes (on the logarithmic scale) in each signature gene set, as previously described<sup>24,29</sup>.

Profiled tumor RNA sequencing samples were assigned to molecular subtypes according to the transcriptomically defined clustering in the phase 3 IMmotion151 trial of atezolizumab plus bevacizumab as first-line therapy compared to sunitinib in participants with advanced or metastatic RCC<sup>8</sup>. The molecular subtypes were assigned as follows. First, tumors with an angiogenesis consensus signature score above the upper tertile were assigned to the angiogenic group. Second, among tumors assigned to the angiogenic group, those that had a stroma/EMT/TGF $\beta$  consensus signature score above the median (evaluated over all samples) were assigned to the angiogenic–stromal group. Third, among the remaining samples, those that had a Tcell<sub>inf</sub>GEP score above the 75th percentile (evaluated over all samples) were assigned to the immune–proliferative group. Fourth, among the remaining (yet unassigned to the other groups) samples, those with a low proliferation consensus signature score (defined for which the proliferation score was below the lower tertile (evaluated over the not-already-assigned samples)) were assigned to the ‘other’ group. Finally, among the remaining samples, those for which a stroma/EMT/TGF $\beta$  score was higher than the median (evaluated over the remaining samples) were assigned to the stromal–proliferative group, whereas the other half was assigned to the proliferative group.

WES was performed on FFPE sections of pretreatment tumor samples and on matched normal (blood cell) samples using ACE Cancer Exome technology (Personalis), with average coverage of 200 $\times$  (range, 13–475)<sup>23,46</sup>. WES reads were aligned to the Genome Reference Consortium Human Build 37 assembly by use of the Burrows–Wheeler Aligner MEM algorithm, followed by preprocessing steps that included duplicate marking, indel realignment and base recalibration using Picard (version 1.114; Broad Institute) and generation of analysis-ready binary alignment map files using Genome Analysis Toolkit (version 2; Broad Institute) analysis software. Thereafter, somatic single-nucleotide variant (SNV) calls were generated by



comparing binary alignment map files from tumor and matched normal samples using default parameters from the MuTect method<sup>47</sup>. MuTect-called SNVs that were present in the Single Nucleotide Polymorphism Database (version 141; National Center for Biotechnology Information, <https://www.ncbi.nlm.nih.gov/snp/>) but not in the Catalogue of Somatic Mutations in Cancer (version 68; <http://cancer.sanger.ac.uk>) were filtered out<sup>48</sup>. SNVs with mutant reads of fewer than four in tumor samples were also eliminated. MuTect2 was further used to comprehensively characterize insertion or deletion–spliced mutations.

### Statistical analysis

We assessed efficacy in the intention-to-treat population, which included all randomly assigned participants, and followed guidelines published previously<sup>2,31</sup>. Because the trial outcome was previously defined as positive and the present analysis is exploratory, no formal hypothesis testing was performed in the present analysis. In the biomarker analysis population, we included all participants who received at least one dose of study treatment and had available PD-L1, RNA sequencing or WES data that passed quality control.

We used the Kaplan–Meier method to estimate OS, PFS and DOR in each treatment arm. To estimate the magnitude of the treatment difference (that is, hazard ratio) between the treatment arms, we used a stratified Cox proportional hazards model with the Efron method for handling ties. The stratification factors used for randomization were applied to the stratified Cox model. The stratified Miettinen and Nurminen method, with weights proportional to the stratum size, was used for comparison of ORR between the treatment arms. For ORR, 95% confidence intervals were based on the binomial exact confidence interval method for binomial data. Additionally, we assessed OS and PFS in protocol-prespecified subgroups based on participants' baseline characteristics, including IMDC risk category and PD-L1 status. Post hoc analysis of efficacy was also performed for participants who completed 35 cycles of pembrolizumab. No formal hypothesis testing was conducted for the follow-up analysis of efficacy.

The biomarker analysis followed a statistical analysis plan written before merging of the clinical data with biomarker assessment, specifying where statistical testing would be used and what biomarker cutoffs defined the subgroups for treatment arm comparisons. The association between each biomarker and the clinical outcomes with pembrolizumab plus axitinib or sunitinib was assessed using logistic regression for ORR or a Cox proportional hazards regression model for OS and PFS. All models were adjusted by IMDC risk category, as prespecified in the statistical analysis plan. Statistical significance for associations between biomarkers and clinical outcomes (ORR, OS and PFS) was prespecified at  $\alpha < 0.05$  (without multiplicity adjustment) for Tcell<sub>inf</sub>GEP, the angiogenesis signature and PD-L1 CPS separately; at  $\alpha < 0.10$  after multiplicity adjustment (Hochberg step-up procedure; tested as one family of 10 hypotheses (before Tcell<sub>inf</sub>GEP adjustment) or nine hypotheses (after Tcell<sub>inf</sub>GEP adjustment) within each treatment arm) for the other signatures and molecular subtypes; and at  $\alpha < 0.10$  after multiplicity adjustment for DNA mutations, as prespecified in the statistical analysis plan. The direction of the hypothesis tests (that is, non-zero association (two-tailed test), positive association or negative association (one-tailed test)) for the Tcell<sub>inf</sub>GEP and other signatures was informed by an internal evaluation of published data from other trials, including the phase 3 JAVELIN Renal 101 trial of avelumab plus axitinib compared to sunitinib in participants with previously untreated advanced RCC<sup>9,11</sup>. The Spearman correlation was used to evaluate the relationship between pairs of RNA signatures and (or) biomarkers. Using prespecified cutoffs for the Tcell<sub>inf</sub>GEP ( $\geq$  first tertile (Tcell<sub>inf</sub>GEP<sup>non-low</sup>) and  $<$  first tertile (Tcell<sub>inf</sub>GEP<sup>low</sup>) as previously defined and validated using pan-tumor clinical data<sup>23,49</sup>) and angiogenesis signature ( $\geq$  median and  $<$  median; the choice of median as the cutoff was for illustrative purposes) and mutational status (mutant versus wild-type) for *VHL*, *PBRM1*, *SETD2*

and *BAP1*, we performed descriptive subgroup analyses to estimate OS and PFS benefits of pembrolizumab plus axitinib compared to sunitinib and to assess the relative prognostic and predictive effects of the biomarkers. Statistical analyses were performed in SAS version 9.4 and R version 4.2.1 software. The data cutoff for this analysis was 23 January 2023.

### Reporting summary

Further information on research design is available in the Nature Portfolio Reporting Summary linked to this article.

### Data availability

Merck Sharp & Dohme (MSD), a subsidiary of Merck & Co., is committed to providing qualified scientific researchers access to anonymized data and clinical study reports from the company's clinical trials for the purpose of conducting legitimate scientific research. MSD is also obligated to protect the rights and privacy of trial participants and, as such, has a procedure in place for evaluating and fulfilling requests for sharing company clinical trial data with qualified external scientific researchers. The MSD data-sharing website (<https://externaldatasharing-msd.com/>) outlines the process and requirements for submitting a data request. Applications will be promptly assessed for completeness and policy compliance. Feasible requests will be reviewed by a committee of MSD subject matter experts to assess the scientific validity of the request and the qualifications of the requestors. In line with data privacy legislation, submitters of approved requests must enter into a standard data-sharing agreement with MSD before data access is granted. Data will be made available for request after product approval in the United States and the European Union or after product development is discontinued. Certain circumstances may prevent MSD from sharing requested data, including country-specific or region-specific regulations. If the request is declined, it will be communicated to the investigator. Access to genetic or exploratory biomarker data requires a detailed, hypothesis-driven statistical analysis plan that is collaboratively developed by the requestor and MSD subject matter experts; after approval of the statistical analysis plan and execution of a data-sharing agreement, MSD will either perform the proposed analyses and share the results with the requestor or will construct biomarker covariates and add them to a file with clinical data that is uploaded to an analysis portal so that the requestor can perform the proposed analyses.

### References

- US Department of Health and Human Services. Guidance for industry: clinical trial endpoints for the approval of cancer drugs and biologics (2018).
- Hu, J., Ge, H., Newman, M. & Liu, K. OSA: a fast and accurate alignment tool for RNAseq. *Bioinformatics* **28**, 1933–1934 (2012).
- Li, B. & Dewey, C. N. RSEM: accurate transcript quantification from RNA-seq data with or without a reference genome. *BMC Bioinformatics* **12**, 323 (2011).
- Cristescu, R. et al. Tumor mutational burden predicts the efficacy of pembrolizumab monotherapy: a pan-tumor retrospective analysis of participants with advanced solid tumors. *J. Immunother. Cancer* **10**, e003091 (2022).
- Cibulskis, K. et al. Sensitive detection of somatic point mutations in impure and heterogeneous cancer samples. *Nat. Biotechnol.* **31**, 213–219 (2013).
- Bamford, S. et al. The COSMIC (Catalogue of Somatic Mutations in Cancer) database and website. *Br. J. Cancer* **91**, 355–358 (2004).
- Ayers, M. et al. Molecular profiling of cohorts of tumor samples to guide clinical development of pembrolizumab as monotherapy. *Clin. Cancer Res.* **25**, 1564–1573 (2019).



## Acknowledgements

We thank the participants, their families and caregivers for their involvement in this trial as well as all investigators and site personnel. Medical writing and (or) editorial assistance was provided by O. T. Ezeokoli and R. Steger of ApotheCom. This assistance was funded by Merck Sharp & Dohme, a subsidiary of Merck & Co. This work was supported by Merck Sharp & Dohme. The sponsor played a role in the design and conduct of the study; the collection, management, analysis and interpretation of the data; and the preparation, review and approval of the paper.

## Author contributions

B.I.R., E.R.P., D.S., S.W., A.L., R.F.P., J. Burgents and T.P. conceptualized the study. B.I.R., E.R.P., V.S., R.G., T.W., D.N., F.P., B.A., B.M., I.V., S.J.d.A., R.S.M., J. Bedke, S.W. and T.P. contributed to the acquisition of the data. B.I.R., E.R.P., R.G., T.W., F.P., B.A., B.M., J. Bedke, S.W., J.M. and A.V. curated the data. B.I.R., D.N., R.G., T.W., D.S., B.M., S.J.d.A., D.B., S.W., J.M., Y.Z., A.V. and T.P. analyzed and interpreted the data. B.I.R., E.R.P., T.W., D.S., S.W., Y.Z., A.L., A.V., R.F.P., J. Burgents and T.P. contributed to the study methodology. A.V. provided software. D.S., S.T. and J.M. administered the project. B.A. and J. Bedke contributed to funding acquisition. B.A., B.M. and J. Bedke provided resources. B.I.R., E.R.P., T.W., B.A., D.S., J. Bedke, S.T., A.L., R.F.P. and J. Burgents supervised the study. B.I.R., V.S., T.W., F.P., B.A., D.S., B.M., S.J.d.A. and J. Bedke validated the results. B.I.R., B.A., D.S., J. Bedke, Y.Z. and A.V. contributed to data visualization. B.I.R., D.S., A.V. and T.P. wrote the original draft of the paper. All authors reviewed or edited the paper for important intellectual content and approved the final draft for publication.

## Competing interests

B.I.R. reports receiving writing support for the present paper from Merck Sharp & Dohme (MSD); payment to his institution for clinical trial research from MSD; and consulting fees from MSD. E.R.P. reports receiving honoraria for scientific advisory from 23andMe, AbbVie, Adaptimmune, Astellas, AstraZeneca, Aura Biosciences, Bristol Myers Squibb, Daiichi Sankyo, Eisai, EMD Serono, Exelixis, IMV, Merck, Pfizer, Seagen, Seattle Genetics, Signatera, Synthekine, 23andMe and UroGen and continuing medical education talks for Cancer Network Readout 360, Clinical Care Options, CUA, Everyday Health Med Page Today, GU Oncology Now, Mashup Media, Mayo Clinic Hematology–Oncology Reviews, MJH Oncology, OncLive, PlatformQ, Research to Practice, Targeted Oncology, TouchME and VJ Oncology. V.S. reports receiving honoraria for presentations by Pfizer and support for attending meetings and (or) travel from Bionorica. R.G. reports funding for the present paper from MSD; grants or contracts to him and his institution from Astellas, AstraZeneca, Bristol Myers Squibb, Bayer, Ipsen, Janssen, Pfizer and Roche; payment or honoraria for lectures, presentations, speakers' bureaus, paper writing or educational events from Astellas, AstraZeneca, Bristol Myers Squibb, Bayer, Ipsen, Janssen, Pfizer and Roche; support for attending meetings and (or) travel from Astellas, AstraZeneca, Bristol Myers Squibb, Bayer, Ipsen, Janssen, Pfizer and Roche; and participation on a data safety monitoring board or advisory board for Astellas, AstraZeneca, Bristol Myers Squibb, Bayer, Ipsen, Janssen, Pfizer and Roche. T.W. reports a research grant paid to his institution from MSD; honoraria for lectures, presentations, speakers' bureaus, paper writing or educational events from Bristol Myers Squibb, EUSA Pharma, Ipsen and Pfizer; travel support from Bristol Myers Squibb, EUSA Pharma and Ipsen; and advisory board fees from Bristol Myers Squibb, Eisai, EUSA Pharma, Ipsen and MSD. D.N. reports honoraria for lectures from Astellas, AstraZeneca, Eisai, Pfizer and Roche and honoraria for participation on advisory boards from AstraZeneca,

Pfizer and Roche. F.P. reports grants or contracts for research from Astellas, Janssen, Merck & Co., Novartis, Pfizer, Tersera and Tolmar; consulting fees from Astellas, Bayer, Janssen, Novartis, Tersera and Tolmar; payment or honoraria for lectures, presentations, speakers' bureaus, paper writing or educational events from Astellas, Bayer, Janssen, Novartis, Tersera and Tolmar; support for attending meetings and (or) travel from Novartis, Tersera and Tolmar; and leadership or fiduciary role for the National Cancer Institute Prostate Cancer Task Force and the Canadian Cancer Trials Group Genito-Urinary Clinical Trial Group. B.A. reports support for the present paper from MSD; grants or contracts from Astellas, AstraZeneca, Bayer, Bristol Myers Squibb, Eisai, Ipsen, Janssen, Merck & Co., Pfizer and Roche; consulting fees from Astellas, AstraZeneca, Bayer, Eisai, Ipsen, Janssen, Merck & Co., MSD, Pfizer and Roche; payment or honoraria for lectures, presentations, speakers' bureaus, paper writing or educational events from Astellas, AstraZeneca, Bayer, Eisai, Ipsen, Janssen, Merck & Co., MSD, Pfizer and Roche; support for attending meetings and (or) travel from Astellas, AstraZeneca, Bayer, Eisai, Ipsen, Janssen, Merck & Co. and Roche; and participation on a data safety monitoring board or advisory board for Astellas, AstraZeneca, Bayer, Eisai, Ipsen, Janssen, Merck & Co., Pfizer and Roche. D.S. reports support for the present paper from MSD; grants to his institution from Bristol Myers Squibb, Merck & Co. and Novartis; consulting fees from Bristol Myers Squibb, Eisai, Ipsen, Merck & Co. and Pfizer; and payment or honoraria for lectures, presentations, speakers' bureaus, paper writing or educational events from Bristol Myers Squibb, Merck & Co. and Pfizer. B.M. reports receiving honoraria for participation on advisory boards from Astellas, AstraZeneca, Bristol Myers Squibb, Eli Lilly, Eisai, Merck Serono, MSD, Novartis, Pfizer, Pierre Fabre, Roche and Servier; honoraria for lectures from Astellas, AstraZeneca, Bristol Myers Squibb, Eli Lilly, Eisai, Merck Serono, MSD, Novartis, Pfizer, Pierre Fabre, Roche and Servier; and support for attending meetings and (or) travel from AstraZeneca, Bristol Myers Squibb, Merck Serono and MSD. D.B. reports grants to her institution from Bristol Myers Squibb and Pfizer; grants or contracts to her institution for clinical trials from Aveo, Bristol Myers Squibb, Exelixis, MSD, Roche and Pfizer; consulting fees for consulting or advisory board from Bristol Myers Squibb, Ipsen, MSD and Pfizer; and support for traveling to meetings from Ipsen, MSD and Pfizer. R.S.M. reports payment or honoraria for lectures, presentations, speakers' bureaus, paper writing or educational events from Astellas, Bristol Myers Squibb, Ipsen, Janssen and MSD and support for attending meetings and (or) travel from Bayer, Novartis and Pfizer. J. Bedke reports payment or honoraria for lectures, presentations, speakers' bureaus, paper writing or educational events from Apogepha, Astellas, Bristol Myers Squibb, Eisai, F. Hoffman-La Roche, Gilead Sciences, Ipsen Innovation, Janssen, Merck KGaA, MSD, Pfizer and Seagen. S.T. reports payment or honoraria for lectures, presentations, speakers' bureaus, paper writing or educational events from Merck Biopharma, MSD, Pfizer and Takeda. S.W., J.M., Y.Z., A.L., A.V., R.F.P. and J. Burgents are employees of MSD, a subsidiary of Merck & Co., and own stock in Merck & Co. T.P. reports grants or contracts from AstraZeneca, Roche, Bristol Myers Squibb, Exelixis, Ipsen, MSD, Novartis, Pfizer, Seattle Genetics, Merck Serono, Astellas, Johnson & Johnson and Eisai; consulting fees and honoraria from AstraZeneca, Bristol Myers Squibb, Exelixis, Incyte, Ipsen, MSD, Novartis, Pfizer, Seattle Genetics, Merck Serono, Astellas, Johnson & Johnson, Eisai, Roche, Mashup and Gilead Sciences; support for attending meetings and (or) travel from Roche, Pfizer, MSD, AstraZeneca, Ipsen, Gilead Sciences, Astellas and MSD; participation on a data safety monitoring board or advisory board for AstraZeneca, Roche, Bristol Myers Squibb, Exelixis, Ipsen, MSD, Novartis, Pfizer, Seattle Genetics, Merck Serono, Astellas, Johnson

& Johnson and Eisai; and other financial interests from Novartis, Pfizer, AstraZeneca, Roche/Genentech, Eisai and Merck. I.V. and S.J.d.A. declare no competing interests.

### Additional information

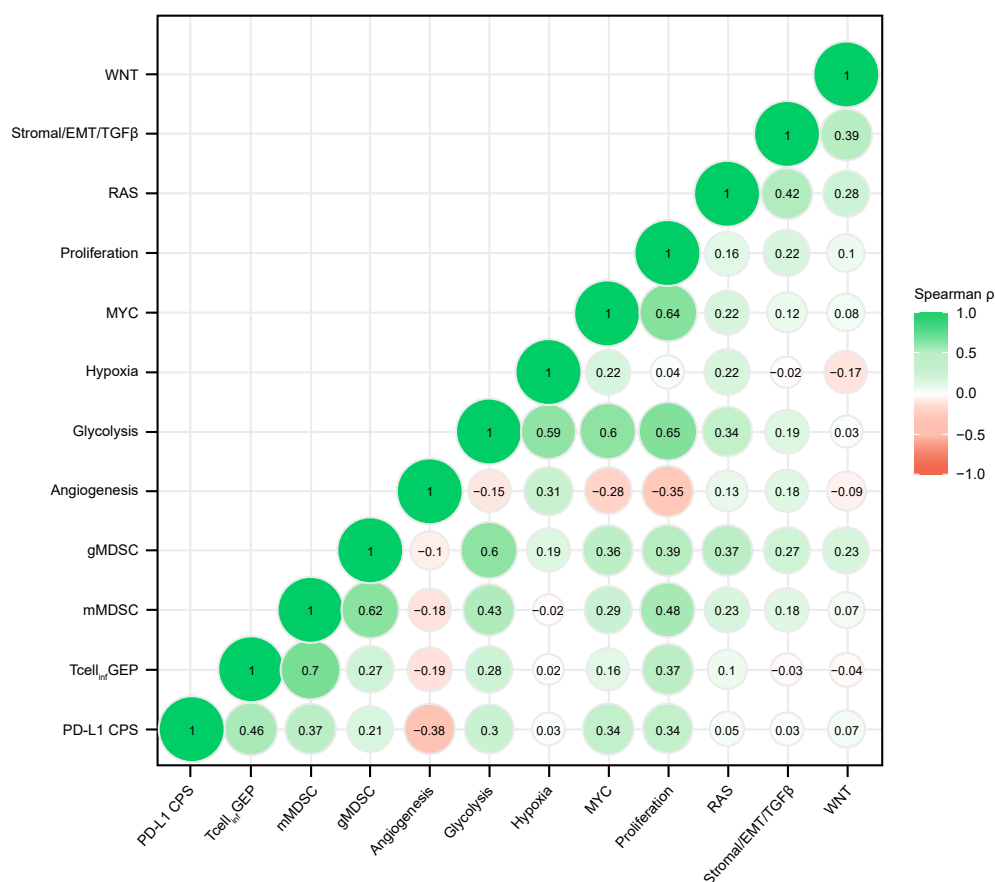
**Extended data** is available for this paper at <https://doi.org/10.1038/s41591-025-03867-5>.

**Supplementary information** The online version contains supplementary material available at <https://doi.org/10.1038/s41591-025-03867-5>.

**Correspondence and requests for materials** should be addressed to Brian I. Rini.

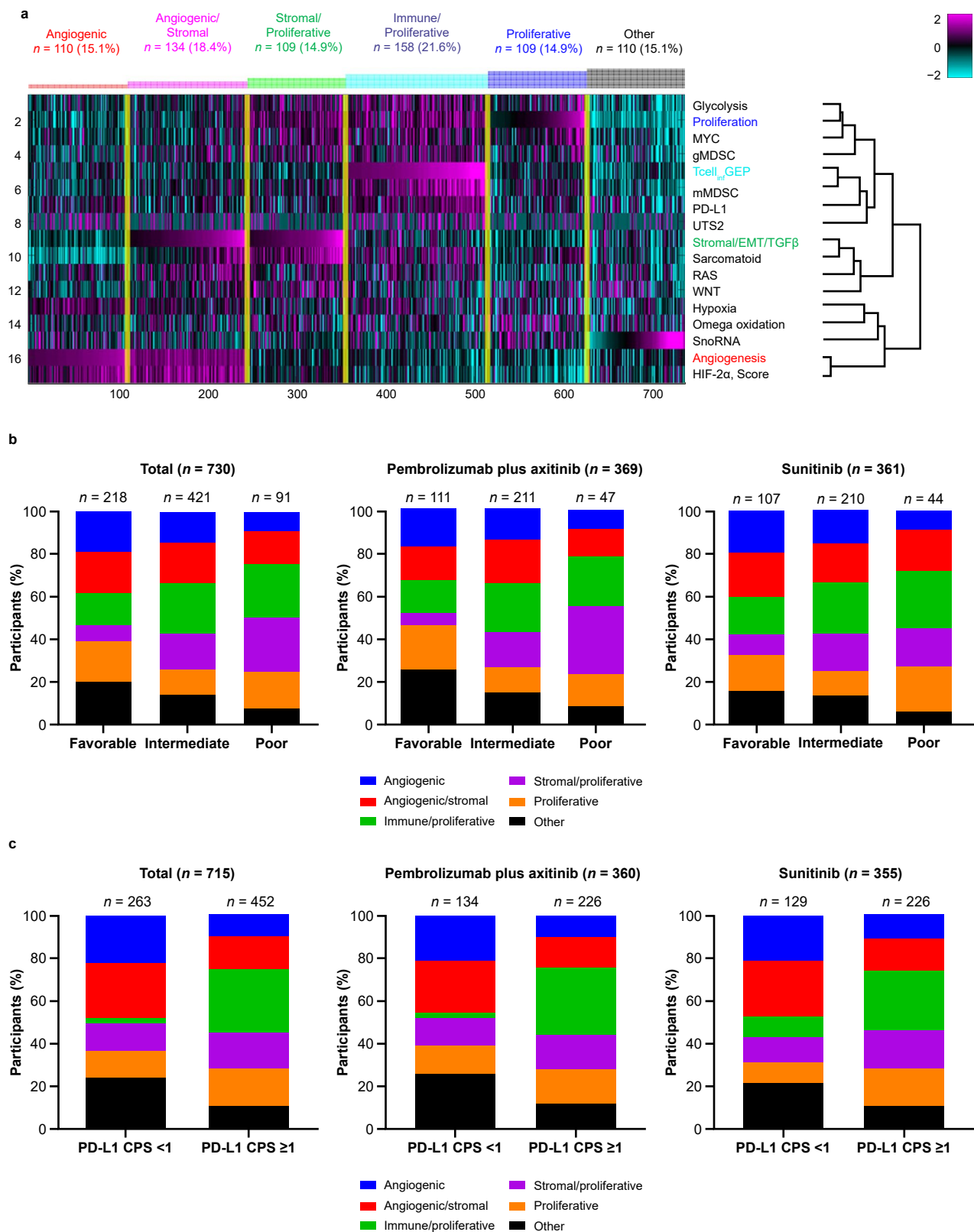
**Peer review information** *Nature Medicine* thanks Ganessan Kichenadasse and the other, anonymous, reviewer(s) for their contribution to the peer review of this work. Primary Handling Editor: Ulrike Harjes, in collaboration with the *Nature Medicine* team.

**Reprints and permissions information** is available at [www.nature.com/reprints](http://www.nature.com/reprints).



**Extended Data Fig. 1 | Correlogram plot of PD-L1 CPS, RNA sequencing signatures, and single genes.** CPS, combined positive score; EMT, epithelial-to-mesenchymal transition; gMDSC, granulocytic myeloid-derived suppressor

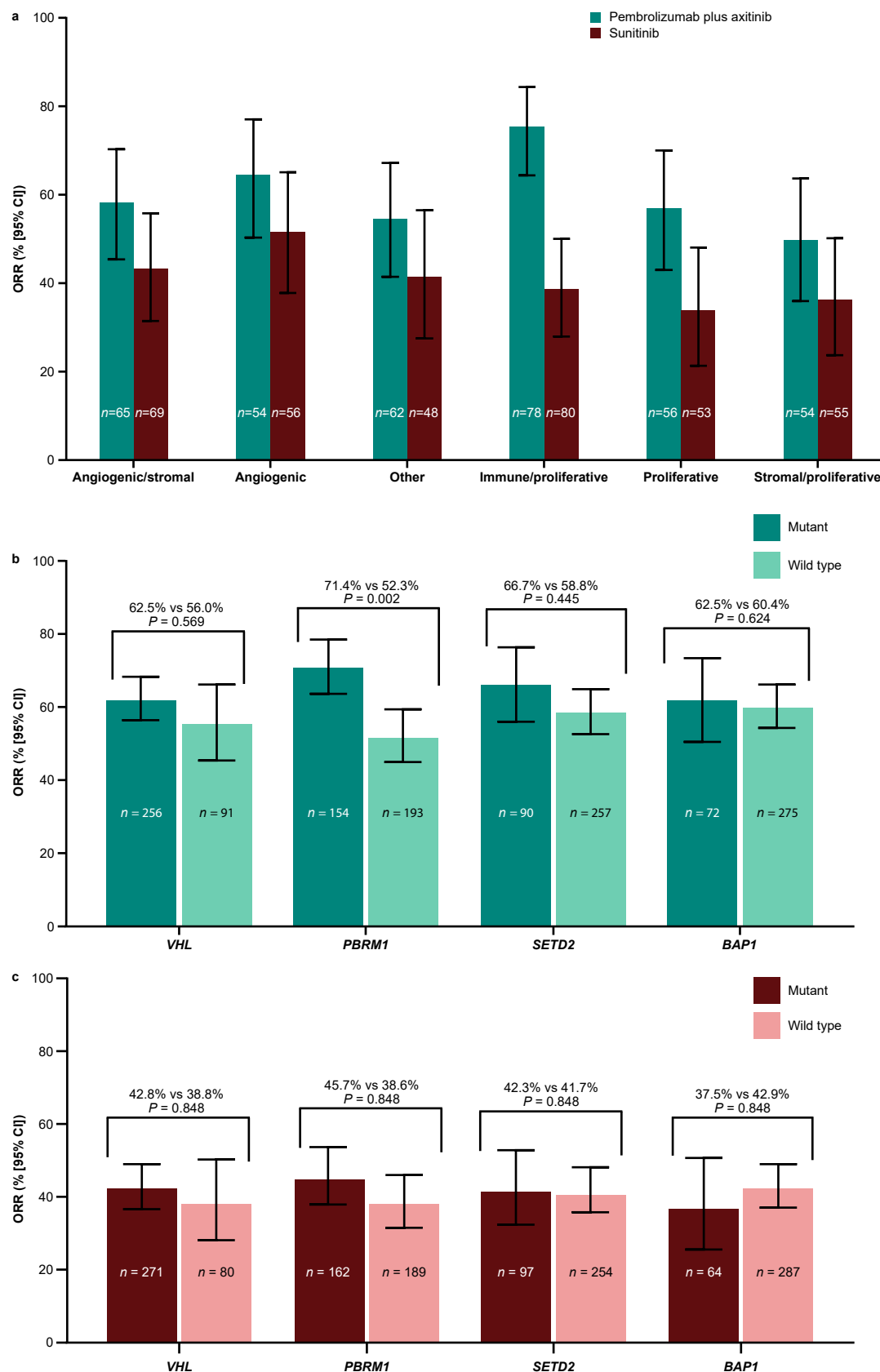
cell; mMDSC, monocytic myeloid-derived suppressor cell; PD-L1, programmed cell death ligand 1; Tcell<sub>infl</sub>GEP, T-cell-inflamed gene expression profile; TGF-β, transforming growth factor β.

**Extended Data Fig. 2 | Clustering and distribution of molecular subtypes.**

**a**, Molecular subtype clustering. **b**, Distribution by IMDC risk categories. **c**, Distribution by tumor PD-L1 CPS. Molecular subtypes are based on transcriptomically defined clustering patterns identified in the IMmotion151 phase 3 study<sup>8</sup>. “Other” includes samples that could not be assigned to the angiogenic/stromal, angiogenic, immune/proliferative, proliferative, or

stromal/proliferative subtype. CPS, combined positive score; EMT, epithelial-to-mesenchymal transition; gMDSC, granulocytic myeloid-derived suppressor cell; HIF-2 $\alpha$ , hypoxia-inducible factor- $\alpha$ ; IMDC, International Metastatic Renal Cell Carcinoma Database Consortium; mMDSC, monocytic myeloid-derived suppressor cell; PD-L1, programmed cell death ligand 1; Tcell<sub>infl</sub>GEP, T-cell-inflamed gene expression profile; TGF- $\beta$ , transforming growth factor  $\beta$ .



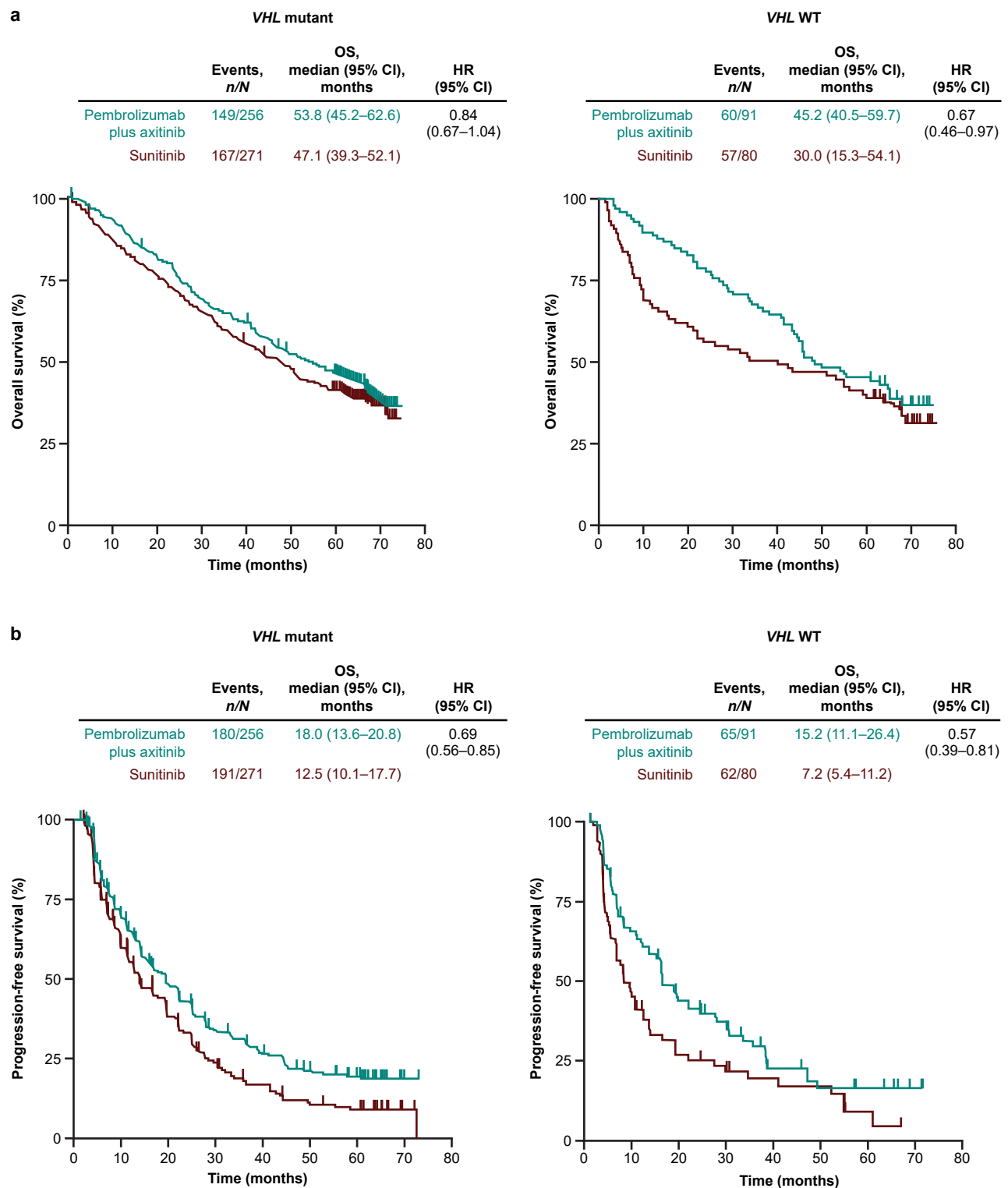


Extended Data Fig. 3 | See next page for caption.

**Extended Data Fig. 3 | ORR by molecular subtypes and mutational status.**

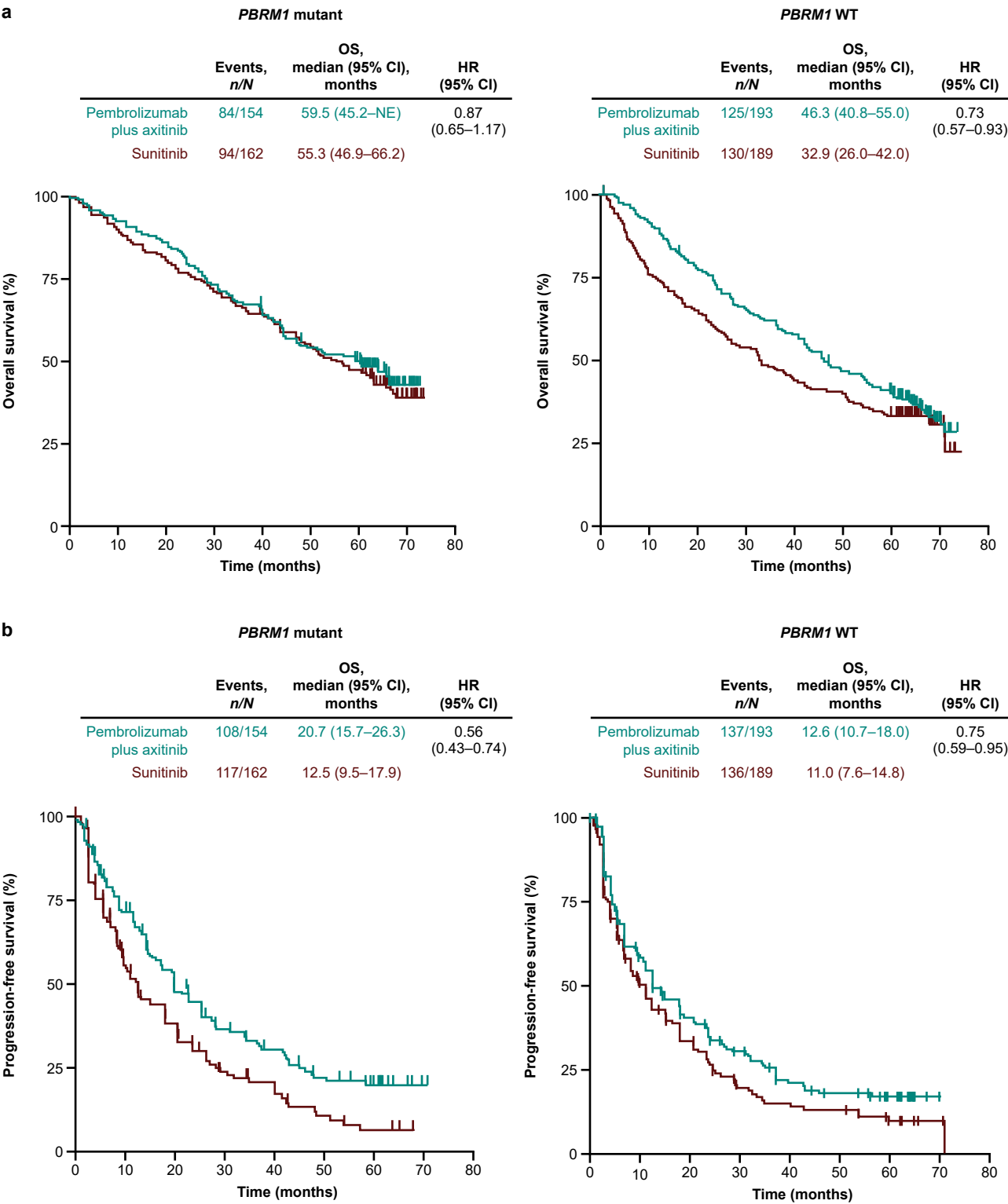
**a**, ORR per transcriptomically defined clustering pattern identified in the IMmotion151 phase 3 study<sup>8</sup> (pembrolizumab plus axitinib,  $n = 369$ ; sunitinib,  $n = 361$ ). **b**, ORR by mutational status in the pembrolizumab plus axitinib arm ( $n = 347$ ). **c**, ORR by mutational status in the sunitinib arm ( $n = 351$ ). In panel **a**, “Other” includes samples that could not be assigned to angiogenic/stromal, angiogenic, immune/proliferative, proliferative, or stromal/proliferative subtype. In panels **a–c**, bars represent ORR, derived by dividing the number of participants with a complete or partial response by the total number of patients

in that subgroup, multiplied by 100. Error bars indicate 95% confidence intervals. *P* values shown in panels **b** and **c** are multiplicity-adjusted (one-sided for pembrolizumab plus axitinib and two-sided for sunitinib) and were derived using logistic regression model, with adjustment for IMDC risk category. Significance was prespecified at  $\alpha = 0.10$ . *BAP1*, *BRCAl*-associated protein 1 gene; IMDC, International Metastatic Renal Cell Carcinoma Database Consortium; NS, not significant; ORR, objective response rate; *PBRM1*, polybromo-1 gene; *SETD2*, SET domain containing 2, histone lysine methyltransferase gene; *VHL*, von Lindau-Hippel tumor suppressor gene.



**Extended Data Fig. 4 | Kaplan-Meier estimates of survival by *VHL* mutational status. **a**, Overall survival. **b**, Progression-free survival. HR was estimated using a Cox proportional hazards model, with adjustment for IMDC risk category. Tick marks represent censored data. HR, hazard ratio; IMDC, International**

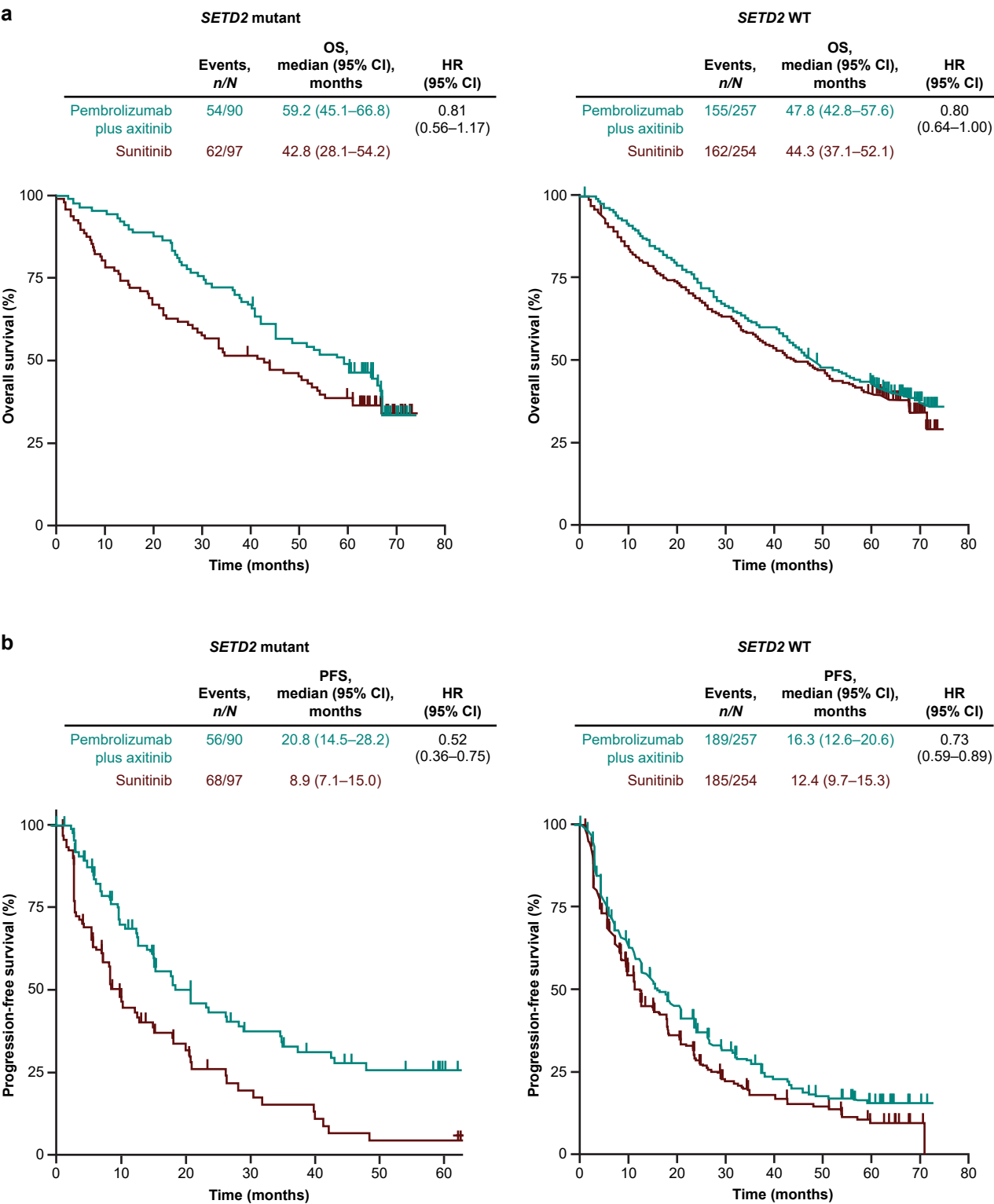
Metastatic Renal Cell Carcinoma Database Consortium; OS, overall survival; PFS, progression-free survival; *VHL*, von Lindau-Hippel tumor suppressor gene; WT, wild type.



**Extended Data Fig. 5 | Kaplan-Meier estimates of survival by *PBRM1* mutational status. **a**, Overall survival. **b**, Progression-free survival. HR was estimated using the Cox proportional hazards model, with adjustment for**

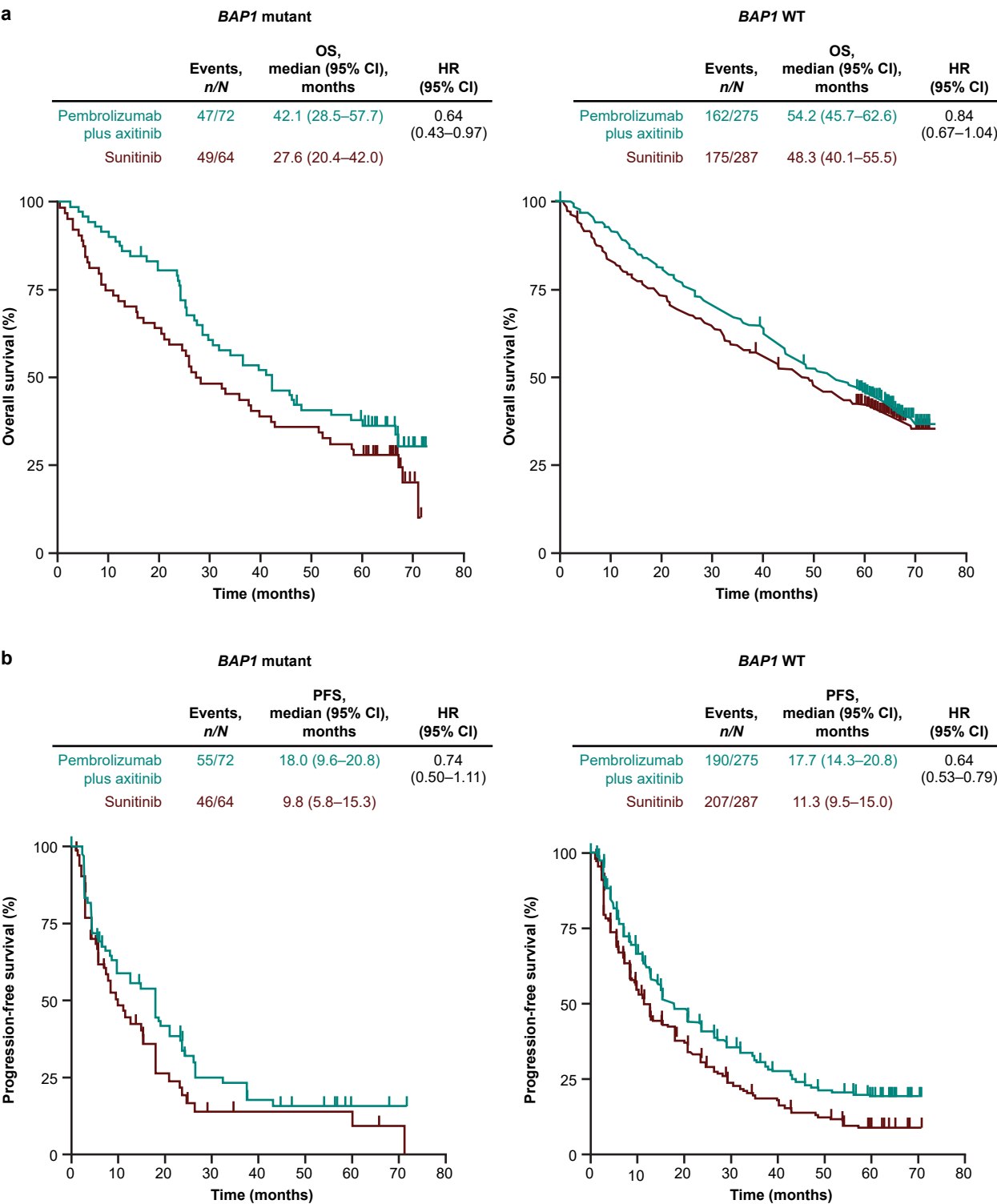
IMDC risk category. HR, hazard ratio; IMDC, International Metastatic Renal Cell Carcinoma Database Consortium; NE, not evaluable; OS, overall survival; *PBRM1*, polybromo-1 gene; PFS, progression-free survival; WT, wild type.





**Extended Data Fig. 6 | Kaplan-Meier estimates of survival by *SETD2* mutational status. **a**, Overall survival. **b**, Progression-free survival. HR was estimated using the Cox proportional hazards model, with adjustment for IMDC risk category.**

HR, hazard ratio; IMDC, International Metastatic Renal Cell Carcinoma Database Consortium; OS, overall survival; PFS, progression-free survival; *SETD2*, SET domain containing 2, histone lysine methyltransferase gene; WT, wild type.



**Extended Data Fig. 7 | Kaplan-Meier estimates of survival by *BAP1* mutational status. **a**, Overall survival. **b**, Progression-free survival. HR was estimated using the Cox proportional hazards model, with adjustment for IMDC risk category.**

*BAP1*, *BRCA1*-associated protein 1 gene; HR, hazard ratio; IMDC, International Metastatic Renal Cell Carcinoma Database Consortium; OS, overall survival; PFS, progression-free survival; WT, wild type.

**Extended Data Table 1 | Summary of confirmed objective response per RECIST v1.1 by BICR in the intention-to-treat population**

	<b>Pembrolizumab plus axitinib <i>n</i> = 432</b>	<b>Sunitinib <i>n</i> = 429</b>
ORR, <sup>a</sup> % (95% CI)	60.6 (55.9–65.3)	39.6 (35.0–44.4)
Estimated treatment difference, <sup>b</sup> % (95% CI)	21.1 (14.6–27.4)	
Best objective response, <i>n</i> (%)		
Complete response	50 (11.6)	17 (4.0)
Partial response	212 (49.1)	153 (35.7)
Stable disease	98 (22.7)	153 (35.7)
Progressive disease	50 (11.6)	73 (17.0)
Not evaluable	6 (1.4)	6 (1.4)
No assessment	16 (3.7)	27 (6.3)

Percentages may not total 100 because of rounding. <sup>a</sup>Includes participants who experienced complete response or partial response. <sup>b</sup>Calculated based on the Miettinen and Nurminen method stratified by IMDC risk group (favorable versus intermediate versus poor) and geographic region (North America versus Western Europe versus rest of the world). <sup>c</sup>Includes participants with postbaseline assessments available but not evaluable (that is, all postbaseline assessments with insufficient data for assessment of response per RECIST v1.1 or complete response, partial response or stable disease <6 weeks from randomization). <sup>d</sup>Includes participants with no postbaseline assessment available for response evaluation.

**Extended Data Table 2 | Within-arm association *P* values between gene expression signatures and molecular subtype and clinical outcomes, after adjustment for Tcell<sub>int</sub>GEP and/or angiogenesis signature**

	Pembrolizumab plus axitinib <i>n</i> = 369			Sunitinib <i>n</i> = 361		
	ORR	PFS	OS	ORR	PFS	OS
Adjusted for Tcell <sub>int</sub> GEP <sup>a</sup>						
Glycolysis	0.840	0.855	0.971	0.579	0.986	0.144
gMDSC	0.840	0.855	0.652	0.579	0.986	0.167
Hypoxia	0.840	0.855	0.971	<b>0.065(+)</b>	0.986	<b>0.095(+)</b>
mMDSC	0.840	0.855	0.971	0.579	0.986	0.108
MYC	0.840	0.855	0.162	0.579	<b>0.019(–)</b>	<b>1.52 × 10<sup>–4</sup>(–)</b>
Proliferation	0.840	0.855	<b>0.007(–)</b>	0.383	0.321	<b>4.56 × 10<sup>–4</sup>(–)</b>
RAS	0.840	0.855	0.971	0.579	0.986	0.530
Stroma/EMT/TGF-β	0.840	0.855	0.971	0.579	0.986	0.445
WNT	0.840	0.344	0.971	0.579	0.986	0.530
Adjusted for Tcell <sub>int</sub> GEP and angiogenesis signature <sup>b</sup>						
Molecular subtype <sup>c</sup>	0.946	0.482	0.075	0.956	0.913	0.293

Association was evaluated using a logistic regression model (ORR) and a Cox proportional hazards regression model (PFS and OS). In the pembrolizumab plus axitinib arm, a negative association (one-tailed test) was hypothesized for glycolysis, proliferation, RAS and stroma/EMT/TGFβ; non-zero associations (two-tailed test) were hypothesized for the remaining gene expression signatures and molecular subtype. In the sunitinib arm, negative associations (one-tailed test) were hypothesized for glycolysis, gMDSC, MYC, proliferation and RAS; non-zero associations (two-tailed test) were hypothesized for the remaining gene expression signatures and molecular subtype. A ‘+’ or ‘–’ indicates that the observed association is positive or negative, respectively. <sup>a</sup>Bolded *P* values indicate nominal statistical significance ( $\alpha < 0.05$ ) for angiogenesis signature and multiplicity-adjusted (Hochberg step-up procedure; tested as one family of nine hypotheses within each treatment arm) statistical significance ( $\alpha < 0.10$ ) for other signatures; all models include additional covariates of IMDC risk category and Tcell<sub>int</sub>GEP. <sup>b</sup>Bolded *P* values indicate nominal statistical significance ( $\alpha < 0.05$ ); all models include additional covariates of IMDC risk category, Tcell<sub>int</sub>GEP and angiogenesis signature. <sup>c</sup>Likelihood ratio test was performed for molecular subtype by comparing the full model (with molecular subtype) to the reduced model (without molecular subtype).



**Extended Data Table 3 | Within-arm association *P* values between DNA mutational status and clinical outcomes**

	Pembrolizumab plus axitinib <i>n</i> = 347			Sunitinib <i>n</i> = 351		
	ORR	PFS	OS	ORR	PFS	OS
<i>VHL</i>	0.569	0.764	0.365	0.848	0.353	<b>0.040(+)</b>
<i>PBRM1</i>	<b>0.002(+)</b>	0.224	0.231	0.848	0.895	<b>0.010(+)</b>
<i>SETD2</i>	0.445	0.224	0.365	0.848	0.895	0.745
<i>BAP1</i>	0.624	0.309	0.365	0.848	0.895	<b>0.019(-)</b>

Association was evaluated using a logistic regression model (ORR) and a Cox proportional hazards regression model (PFS and OS), with adjustment for IMDC risk category. Biomarkers were coded as 0 for wild-type status and 1 for mutant status. Bolded *P* values indicate multiplicity-adjusted statistical significance ( $\alpha < 0.10$ ). A '+' or '-' indicates that the observed association is positive or negative, respectively. In the pembrolizumab plus axitinib arm, a positive association (one-tailed test) was hypothesized for *SETD2*; non-zero associations (two-tailed test) were hypothesized for other biomarkers. In the axitinib arm, non-zero associations (two-tailed test) were hypothesized for all biomarkers.

Reporting Summary

Nature Portfolio wishes to improve the reproducibility of the work that we publish. This form provides structure for consistency and transparency in reporting. For further information on Nature Portfolio policies, see our [Editorial Policies](#) and the [Editorial Policy Checklist](#).

Statistics

For all statistical analyses, confirm that the following items are present in the figure legend, table legend, main text, or Methods section.

n/a	Confirmed
<input type="checkbox"/>	<input checked="" type="checkbox"/> The exact sample size ( <i>n</i> ) for each experimental group/condition, given as a discrete number and unit of measurement
<input checked="" type="checkbox"/>	<input type="checkbox"/> A statement on whether measurements were taken from distinct samples or whether the same sample was measured repeatedly
<input type="checkbox"/>	<input checked="" type="checkbox"/> The statistical test(s) used AND whether they are one- or two-sided <i>Only common tests should be described solely by name; describe more complex techniques in the Methods section.</i>
<input type="checkbox"/>	<input checked="" type="checkbox"/> A description of all covariates tested
<input type="checkbox"/>	<input checked="" type="checkbox"/> A description of any assumptions or corrections, such as tests of normality and adjustment for multiple comparisons
<input type="checkbox"/>	<input checked="" type="checkbox"/> A full description of the statistical parameters including central tendency (e.g. means) or other basic estimates (e.g. regression coefficient) AND variation (e.g. standard deviation) or associated estimates of uncertainty (e.g. confidence intervals)
<input type="checkbox"/>	<input checked="" type="checkbox"/> For null hypothesis testing, the test statistic (e.g. <i>F</i> , <i>t</i> , <i>r</i> ) with confidence intervals, effect sizes, degrees of freedom and <i>P</i> value noted <i>Give P values as exact values whenever suitable.</i>
<input checked="" type="checkbox"/>	<input type="checkbox"/> For Bayesian analysis, information on the choice of priors and Markov chain Monte Carlo settings
<input checked="" type="checkbox"/>	<input type="checkbox"/> For hierarchical and complex designs, identification of the appropriate level for tests and full reporting of outcomes
<input checked="" type="checkbox"/>	<input type="checkbox"/> Estimates of effect sizes (e.g. Cohen's <i>d</i> , Pearson's <i>r</i> ), indicating how they were calculated

Our web collection on [statistics for biologists](#) contains articles on many of the points above.

Software and code

Policy information about [availability of computer code](#)

Data collection	InForm 7.0 for clincial data analysis
Data analysis	SAS, version 9.4. and R version 4.2.1; OmicSoft Array Suite, version 9 (Qiagen, Hilden, Germany). Picard (version 1.114; Broad Institute, Cambridge, MA). The Genome Analysis Toolkit (version 2; Broad Institute. Single Nucleotide Polymorphism Database (v.141; National Center for Biotechnology Information, Bethesda, MD; <a href="https://www.ncbi.nlm.nih.gov/snp/">https://www.ncbi.nlm.nih.gov/snp/</a> ). Burrows-Wheeler Aligner MEM algorithm. RNA-Seq by Expectation Maximization. OmicSoft Sequence Aligner. Catalogue of Somatic Mutations in Cancer (v.68; <a href="http://cancer.sanger.ac.uk">http://cancer.sanger.ac.uk</a> )

For manuscripts utilizing custom algorithms or software that are central to the research but not yet described in published literature, software must be made available to editors and reviewers. We strongly encourage code deposition in a community repository (e.g. GitHub). See the Nature Portfolio [guidelines for submitting code & software](#) for further information.

Data

Policy information about [availability of data](#)

All manuscripts must include a [data availability statement](#). This statement should provide the following information, where applicable:

- Accession codes, unique identifiers, or web links for publicly available datasets
- A description of any restrictions on data availability
- For clinical datasets or third party data, please ensure that the statement adheres to our [policy](#)

Merck Sharp & Dohme LLC, a subsidiary of Merck & Co., Inc., Rahway, NJ, USA (MSD), is committed to providing qualified scientific researchers access to

anonymized data and clinical study reports from the company's clinical trials for the purpose of conducting legitimate scientific research. MSD is also obligated to protect the rights and privacy of trial participants and, as such, has a procedure in place for evaluating and fulfilling requests for sharing company clinical trial data with qualified external scientific researchers. The MSD data sharing website (available at: <https://externaldatasharing-msd.com/>) outlines the process and requirements for submitting a data request. Applications will be promptly assessed for completeness and policy compliance. Feasible requests will be reviewed by a committee of MSD subject matter experts to assess the scientific validity of the request and the qualifications of the requestors. In line with data privacy legislation, submitters of approved requests must enter into a standard data-sharing agreement with MSD before data access is granted. Data will be made available for request after product approval in the United States and the European Union or after product development is discontinued. There are circumstances that may prevent MSD from sharing requested data, including country or region-specific regulations. If the request is declined, it will be communicated to the investigator. Access to genetic or exploratory biomarker data requires a detailed, hypothesis-driven statistical analysis plan that is collaboratively developed by the requestor and MSD subject matter experts; after approval of the statistical analysis plan and execution of a data-sharing agreement, MSD will either perform the proposed analyses and share the results with the requestor or will construct biomarker covariates and add them to a file with clinical data that is uploaded to an analysis portal so that the requestor can perform the proposed analyses.

## Research involving human participants, their data, or biological material

Policy information about studies with [human participants or human data](#). See also policy information about [sex, gender \(identity/presentation\), and sexual orientation](#) and [race, ethnicity and racism](#).

Reporting on sex and gender	Data regarding sex are provided in the baseline demographics and disease characteristics table (Supplementary Table 1). Overall survival and progression-free survival outcomes by sex are reported in Figure 2. No individual-level data are presented.
Reporting on race, ethnicity, or other socially relevant groupings	No analyses of race, ethnicity, or other socially relevant groups were performed.
Population characteristics	The median age of the overall participant population was 62.0 years. The majority of participants in the overall study population were aged 65 or below (62.5%), male (72.9%), White (79.4%), and non Hispanic Or Latino (88.7%).
Recruitment	Patients who met the eligibility criteria were recruited by study investigators
Ethics oversight	The study was conducted in accordance with principles of Good Clinical Practice and was approved by the appropriate institutional review boards and regulatory agencies. Written informed consent was provided by all participants before enrollment.

Note that full information on the approval of the study protocol must also be provided in the manuscript.

## Field-specific reporting

Please select the one below that is the best fit for your research. If you are not sure, read the appropriate sections before making your selection.

☒ Life sciences ☐ Behavioural & social sciences ☐ Ecological, evolutionary & environmental sciences

For a reference copy of the document with all sections, see [nature.com/documents/nr-reporting-summary-flat.pdf](https://nature.com/documents/nr-reporting-summary-flat.pdf)

## Life sciences study design

All studies must disclose on these points even when the disclosure is negative.

Sample size	Sample size was previously reported in the first interim analysis. We assessed efficacy in the intention-to-treat population, which included all randomly assigned participants, and followed guidelines published previously. 861 participants were randomly assigned to receive either pembrolizumab plus axitinib (n = 432) or sunitinib monotherapy (n = 429)
Data exclusions	We assessed efficacy in the intention-to-treat population, which included all randomly assigned participants. In the biomarker analysis population, we included all participants who received at least one dose of study treatment and had available PD-L1, RNA sequencing, or WES data that passed quality control.
Replication	This was a clinical study so no replication was attempted.
Randomization	Participants were randomly assigned in a 1:1 ratio to receive pembrolizumab 200 mg intravenously once every 3 weeks for up to 35 cycles (~2 years) plus axitinib 5 mg by mouth twice daily continuously or sunitinib 50 mg by mouth once daily for 4 weeks on and 2 weeks off, continuously. Randomization was done using an interactive voice response system or integrated web response system, and was stratified according to the International Metastatic Renal Cell Carcinoma Database Consortium (IMDC) risk group (favorable vs intermediate vs poor risk) and by geographic region (North America vs Western Europe vs rest of the world).
Blinding	This was an open-label study.

## Reporting for specific materials, systems and methods

We require information from authors about some types of materials, experimental systems and methods used in many studies. Here, indicate whether each material, system or method listed is relevant to your study. If you are not sure if a list item applies to your research, read the appropriate section before selecting a response.

## Materials & experimental systems

n/a	Involved in the study
<input checked="" type="checkbox"/>	<input type="checkbox"/> Antibodies
<input checked="" type="checkbox"/>	<input type="checkbox"/> Eukaryotic cell lines
<input checked="" type="checkbox"/>	<input type="checkbox"/> Palaeontology and archaeology
<input checked="" type="checkbox"/>	<input type="checkbox"/> Animals and other organisms
<input type="checkbox"/>	<input checked="" type="checkbox"/> Clinical data
<input checked="" type="checkbox"/>	<input type="checkbox"/> Dual use research of concern
<input checked="" type="checkbox"/>	<input type="checkbox"/> Plants

## Methods

n/a	Involved in the study
<input checked="" type="checkbox"/>	<input type="checkbox"/> ChIP-seq
<input checked="" type="checkbox"/>	<input type="checkbox"/> Flow cytometry
<input checked="" type="checkbox"/>	<input type="checkbox"/> MRI-based neuroimaging

## Clinical data

Policy information about [clinical studies](#)

All manuscripts should comply with the ICMJE [guidelines for publication of clinical research](#) and a completed [CONSORT checklist](#) must be included with all submissions.

Clinical trial registration	Clinicaltrials.gov, NCT02853331
Study protocol	Full protocol has been previously published
Data collection	Patients were enrolled from 129 centers (hospitals and cancer centers) globally between October 2016 and January 2018. For the biomarker analysis, formalin-fixed, paraffin-embedded pretreatment tumor tissue samples collected at screening were used. WES was performed on formalin-fixed paraffin-embedded sections of pretreatment tumor samples and on matched normal (blood cell) samples. RNA sequencing was performed on Illumina HiSeq (Illumina, Inc., San Diego, CA) by use of the TruSeq Access protocol.
Outcomes	<p>The dual primary end points of OS and PFS per RECIST v1.1 by blinded independent central review (BICR) and key secondary end point of ORR per RECIST v1.1 by BICR.</p> <p>The prespecified objectives of the exploratory biomarker analysis, defined in a statistical analysis plan, were as follows:</p> <p>(1) To assess whether an IFN-<math>\gamma</math>-related 18-gene T-cell-inflamed gene expression profile (TcellinfGEP) and 10 other signatures (angiogenesis, glycolysis, granulocytic myeloid-derived suppressor cells [gMDSCs], hypoxia, monocytic myeloid-derived suppressor cells [mMDSCs], MYC, proliferation, RAS, stroma/epithelial-to-mesenchymal transition (EMT)/transforming growth factor <math>\beta</math> [TGF-<math>\beta</math>], and WNT)<sup>20</sup> are individually associated with clinical outcomes (ORR, OS, and PFS) of pembrolizumab plus axitinib or sunitinib;</p> <p>(2) To assess whether prespecified molecular subtypes as categorical variables are separately associated with clinical outcomes of pembrolizumab plus axitinib or of sunitinib;</p> <p>(3) To assess whether continuous PD-L1 combined positive score (CPS) is separately associated with clinical outcomes of pembrolizumab plus axitinib or of sunitinib; and</p> <p>(4) To assess whether mutation status of key RCC driver genes (von Hippel-Lindau tumor suppressor [VHL], PBRM1, SET domain containing 2, histone lysine methyltransferase [SETD2], and BRCA1-associated protein 1 [BAP1]), as determined by whole exome sequencing (WES), are separately associated with clinical outcomes of pembrolizumab plus axitinib or of sunitinib.</p>

## Plants

Seed stocks	NA
Novel plant genotypes	NA
Authentication	NA